UNIVERSITÀ POLITECNICA DELLE MARCHE
DIPARTIMENTO DI SCIENZE DELLA VITA E DELL'AMBIENTE

Corso di Laurea Magistrale in Biologia Marina

Successioni microbiche marine su prototipi di piattaforme petrolifere offshore sottoposti a tecnologia di accrescimento minerale

Marine microbial successions on prototypes of offshore oil and gas platforms under mineral accretion technology

Tesi di Laurea Magistrale di:
Anna Salvatori

_____

Relatore:
Prof.ssa
Cinzia Corinaldesi

_____

Correlatore:
Dott. Stefano Varrella

_____

Sessione Invernale
Anno Accademico 2021/2022

RIASSUNTO

Una delle principali sfide che l'industria globale del petrolio e del gas si troverà ad affrontare nei prossimi anni riguarda la disattivazione delle piattaforme offshore. Le piattaforme offshore hanno un ciclo di vita che va dai 20 ai 40 anni e, al termine del loro sfruttamento, devono essere dismesse. La rimozione completa di queste strutture presenta, tuttavia, costi elevati e notevoli impatti ecologici. Le piattaforme, durante la loro vita produttiva, supportano comunità marine abbondanti e diversificate; possono fornire rifugio per specie sovra sfruttate o minacciate e aumentare la complessità ambientale fornendo un substrato duro aggiuntivo. Inoltre, nei pressi della piattaforma è vietata la pesca commerciale, cosa che fa sì che la struttura funzioni di fatto come un'area marina protetta. È pertanto improbabile che la completa rimozione delle piattaforme estrattive rappresenti la migliore soluzione da un punto di vista ambientale. Lasciare *in situ* le strutture obsolete e convertirle in reef artificiali potrebbe combinare obiettivi economici ed ecologici e rappresentare una valida alternativa. La principale sfida è quella di aumentare la durabilità e la stabilità delle strutture proteggendole dalla corrosione. La soluzione può essere trovata nella tecnologia di accrescimento minerale mediante elettrolisi a bassa tensione di acqua marina che porta alla precipitazione di uno spesso strato di carbonato di calcio al di sopra di strutture metalliche. Questa tecnologia è utilizzata per la

restoration dei coralli e applica lo stesso principio della protezione catodica a corrente impressa, impiegata nella protezione dalla corrosione. Se applicata alle piattaforme offshore dismesse potrebbe fornire maggiore stabilità e proteggerle dalla corrosione. Inoltre, i depositi di carbonato di calcio potrebbero fornire un substrato adatto per la colonizzazione da parte degli organismi marini. I procarioti sono i primi colonizzatori di qualsiasi superficie sommersa attraverso la formazione del biofilm. Le proprietà del biofilm possono influenzare le relazioni trofiche, la colonizzazione e il reclutamento di organismi del macrofouling.

Il presente studio si propone di esplorare e confrontare la diversità microbica (procariotica e fungina) associata a prototipi di piattaforme petrolifere e di gas offshore utilizzando sia analisi tradizionali (microscopia a epifluorescenza) che analisi di metabarcoding (considerando i geni 16S e Internal Transcribed Spacer 2 dell'RNA ribosomiale). I prototipi consistevano in due moduli composti da 8 catodi a forma di barre cilindriche in acciaio; uno dei due moduli è stato sottoposto a tecnologia di accrescimento minerale mentre l'altro è stato usato come controllo. Lo studio ha avuto una durata di dieci mesi. I risultati hanno mostrato che il biofilm sviluppatosi sui prototipi non elettrificati presentava gruppi come *Zetaproteobacteria, Desulfobacterota, Clostridia, Sulfurimonadaceae* e *Arcobacteraceae* normalmente responsabili di corrosione

di strutture metalliche. Questi erano quasi del tutto assenti nei prototipi elettrificati. Ciò potrebbe dimostrare l'efficacia della tecnologia di accrescimento minerale nel fornire protezione contro la corrosione. La comunità fungina si è sviluppata su entrambi i tipi di substrato ma alcuni taxa generalmente parassiti (*Chytridiomycota* e *Rozellomycota*) erano maggiormente presenti nei prototipi non elettrificati suggerendo che l'elettrificazione possa fornire protezione da funghi patogeni agli organismi marini.

Questo studio rappresenta un primo passo verso una migliore comprensione della colonizzazione microbica su prototipi elettrificati che dovrebbe essere presa in considerazione nei prossimi programmi di monitoraggio come indicatore precoce per applicare con successo l'elettrificazione alle piattaforme offshore di petrolio e gas rendendole dei veri e propri reef artificiali.

TABLE OF CONTENTS

1. INTRODUCTION

1.1 Decommissioning of offshore oil and gas platforms: issues and opportunities

One of the major challenges facing the global oil and gas industry in social, environmental, and economic terms is the decommissioning of offshore platforms (Capobianco et al., 2021). Offshore oil and gas platforms have a life cycle between 20 and 40 years (Lakhal et al., 2009). At the end of their exploitation, they will need to be decommissioned (Techera and Chandler, 2015). More than 7500 offshore structures are currently distributed worldwide in 53 different countries (Ferreira and Suslick, 2001). To date, 127 offshore platforms (about 0,4% of the world's oil and gas reserves) are active in the Mediterranean basin, mainly located in the northern and central Adriatic Sea, the central Mediterranean Sea, the Sicily channel, and the Ionian Sea (https://unmig.mise.gov.it; Margheritini et al., 2020). However, over the next decade, most of them will become obsolete and will require to be decommissioned (Parente et al., 2006). Generally, the usual methods of decommissioning involve any of these options: complete removal, partial removal, toppling, and leave-in-place for reefing or re-using the platform (Lakhal et al., 2009). The choice of the complete removal option can have a much wider impact on marine ecosystems (Claisse et al., 2014; Fowler et al.,

2018; Henry et al., 2018). The common practice for platform removal requires explosives or mechanical techniques below the seafloor to demolish the infrastructures (Bull and Love, 2019). This complex process has huge economic costs and also considerable environmental impacts (Lakhal et al., 2009). The equipment used to dismantle and transport the structure, the dispersion of contaminants, the use of explosives, and the consequent removal of no-fishing zones in that area affect air and water quality, the biological communities that have developed on the infrastructure, and fish productivity (Macreadie et al., 2011; Henrion et al., 2015).

The international removal policies are based on the assumption that "leaving the seabed as found" would be the most sustainable option for the marine environment (Margheritini et al., 2020). The legal framework influencing decommissioning includes both international and national law (Techera and Chandler, 2015). The first document about the complete removal of offshore platforms dates back 1958 in the Geneva Convention on the Continental Shelf article 5 (Fowler et al., 2018). It reports that "any installations or structures abandoned or disused must be entirely removed" (Techera and Chandler, 2015). Subsequently, in 1982, with the UNCLOS Convention (United Nations Convention on the Law of the Sea) article 60, some exceptions to the complete removal were introduced (i.e., "partial removal option"; Hamzah, 2003). The

partial removal must guarantee the safety of navigation and environmental protection taking into account IMO (International Maritime Organization) guidelines (Fowler et al., 2018). In 1989, IMO developed the Guidelines and Standards for the Removal of Offshore Installations and Structures on the Continental Shelf and in the Exclusive Economic Zone (Techera and Chandler, 2015). Overall, *in situ* decommissioning is not expressively prohibited and where a "new use" can be identified, countries are not obliged to remove the entire structure (van Elden et al., 2019). The substantial costs of decommissioning and its related environmental issues have led to a gradual change in international regulations toward more flexible approaches (Capobianco et al., 2021). Recently, in Italy, the Ministerial Decree dated 15/02/2019 promoted the reuse of existing platforms, evaluating any innovative alternative (Margheritini et al., 2020). This is in accordance with the latest European economic policies with a view to the circular economy and sustainable growth (Blue Growth Strategy; Margheritini et al., 2020). Leaving in situ the obsolete structures and finding alternative solutions for their sustainable reuse might combine social, ecological, and economic objectives (Capobianco et al., 2021). It can provide considerable cost savings for the oil and gas industry and can be useful to benthic habitat conservation and fishery management (Macreadie et al., 2011). Indeed, from a biological viewpoint,

offshore oil and gas platforms often become key habitats for a vast array of organisms (fishes and invertebrates), including threatened or economically important species (van Elden et al., 2019; Fowler et al., 2018; Figure 1,).

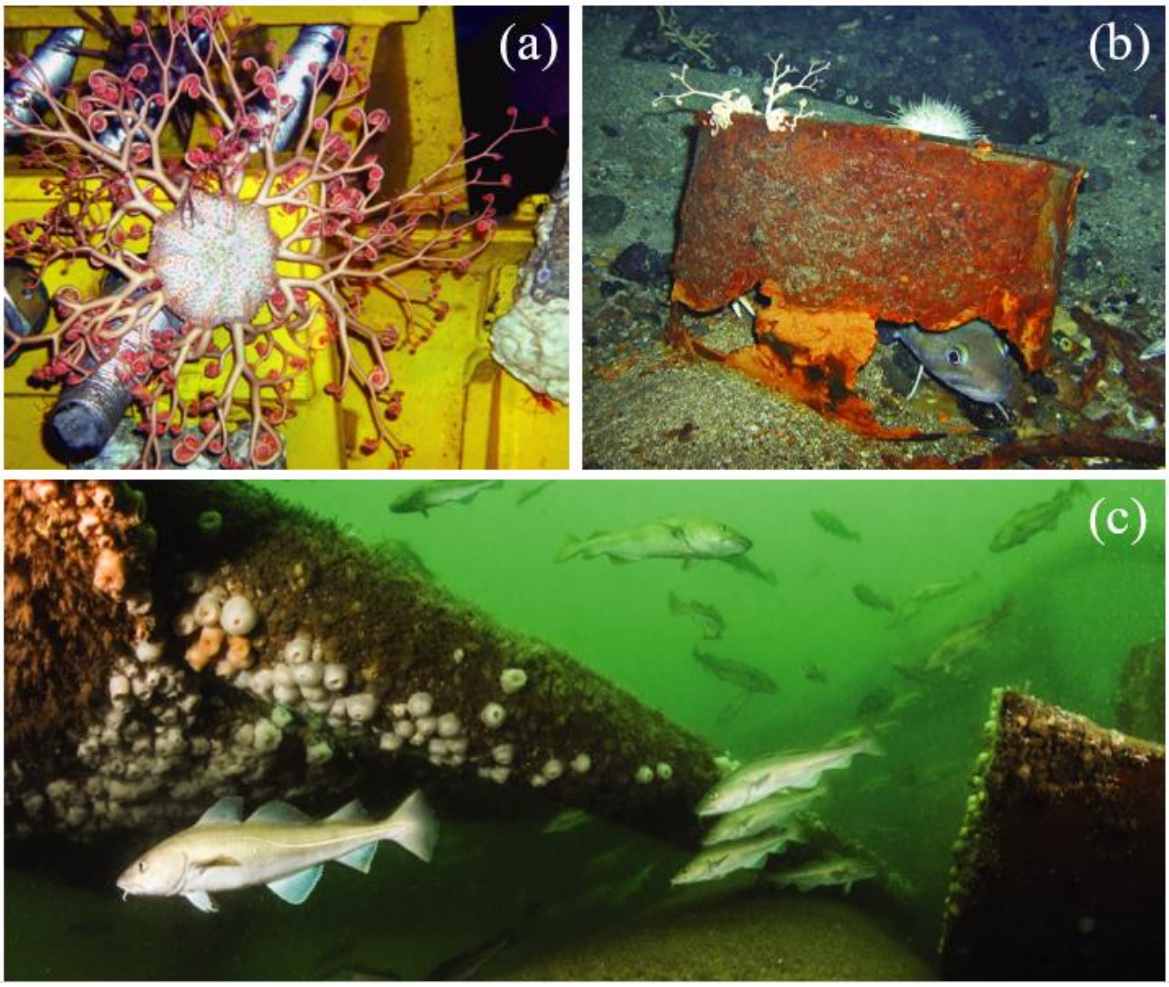

Figure 1. Examples of marine organisms living on oil and gas platforms in the North Sea: (a) a basket star (*Gorgonocephalus caputmedusae*); (b) a rockfish (*Sebastes* sp) with prey; (c) Atlantic cod (*Gadus morhua*). Modified from Fowler et al., 2018.

Schroeder and Love (2004) described oil and gas platforms as "de facto marine protected areas" which offer shelter to marine organisms. These structures create a hard substrate in open waters, suitable for invertebrate colonization and

growth (van Elden et al., 2019). Fabi et al. (2004), after a three-year monitoring of two platforms placed in the northern Adriatic Sea, found higher species richness and greater diversity of fish assemblages induced by the rigs. They observed higher abundances of the poor cod (*Trisopterus minutus capelanus)*, scorpenids associated with large amounts of mussel shells (*Mytilus galloprovincialis*), seabreams (i.e., *Diplodus sargus, D. vulgaris,* and *Spondyliosoma cantharus*), and corbs (*Sciaena umbra* and *Umbrina cirrosa*). In this basin, characterized by homogeneous bottoms, the gas platforms increase the environmental complexity providing an additional habitat for reef-dwelling species (Fabi et al., 2004). In addition, oil rigs exclude commercial fishing (mainly bottom trawling) from these sandy areas, limiting the exploitation of marine resources (Claisse et al., 2014).

Love et al. (2006) estimated that Californian rigs sustained 20% of the juveniles of the IUCN critically endangered Boccaccio rockfish (*Sebastes paucispinis*), while Fowler and Both (2012) found structured populations of the Serranidae *Pseudanthias rubrizonatus* supported by the platforms in North Western Australia.

In light of this, the complete removal of oil and gas platforms may not be the most advantageous option to preserve the marine ecosystem (Henrion et al., 2015). Different alternative ways have been suggested including reconverting

offshore platforms into wind or wave energy projects, solar panel arrays, aquaculture facilities, and artificial reefs (Henrion et al., 2015). To date, in the Gulf of Mexico, more than 500 of the decommissioned platforms, mostly in Louisiana and Texas, have been converted into artificial reefs instead of being brought back to shore for disposal (Bull and Love, 2019).

The main challenge of the reefing option is to guarantee extension of lifetime, protection against corrosion, and the structural stability of the platform (Margheritini et al., 2020). The solution may be found in the mineral accretion technology under low-voltage electrolysis of seawater (Margheritini et al., 2020). It was designed by the architect Wolf Hilbertz, inspired by the fact that organisms (e.g., snails and corals) can make their shells and skeletons from chemicals dissolved in seawater (Strömberg et al., 2010). He developed and patented a way to utilize the process of electroaccumulation of minerals dissolved in seawater to slowly grow rock-solid layers of limestone coatings around a surface (US Patent No. 4246075 (A), 1981). He called this coating "Seacrete" to emphasize the marine origin and the high mechanical resistance of the material (similar to concrete or cement; Goreau and Trench, 2013). This technology is based on the precipitation of a thick layer of calcium carbonate on a conductive metal surface (Hilbertz, 1979). If applied to decommissioned offshore platforms, this technique could supply material with greater rigidity,

stability, and could also offer protection against corrosion (Margheritini et al., 2020). Moreover, calcium carbonate deposits have similar features to natural rocks becoming a suitable substrate for the colonization of marine organisms (Siboni et al., 2009).

1.2 Operating principles and outcomes of the mineral accretion technology under low-voltage electrolysis of seawater

The mineral accretion technology under low-voltage electrolysis of seawater has already been employed for restoring coral reef (Biorock®; Hilbertz and Goreau, 1996). This system allows the deposition of a coating material, composed of natural calcium and magnesium minerals, which, in turn, crystallize through water electrolysis on the electrically charged metal surfaces (Hilbertz, 1979). It is linked to Impressed Current Cathodic Protection methods, developed by G.C. Cox in 1940 for corrosion prevention, widely applied for the protection of pipelines, storage tanks, and underground structures in petroleum and oil industries, and for the protection of concrete structures (Skovhus et al., 2017). Cathodic protection is used to control corrosion of a metal surface by making it the cathode of an electrochemical cell (Skovhus et al., 2017). Mineral accretion technology applies the same principles of Cathodic Protection but with different voltages and current intensities (Margheritini et al., 2020). Both two technologies imply the creation of an electrochemical cell that has three main components: two electrodes (cathode and anode) and the seawater as electrolyte (Hilbertz and Goreau, 1996). This can be achieved either by electrically impressed current or sacrificial anodes or employing them together (Little and Wagner, 1995). The

sacrificial anode is a metal with a more negative electrochemical potential than the cathode and dissolves into the seawater, which act as electrolyte (Liduino et al., 2021). This prompts a faster corrosion of the anode and inhibits corrosion of the cathode (Liduino et al., 2021). Water electrolysis begins when at least 1.23 V of electric potential is supplied and results in the release of H^+ ions at the anode (1) and OH^- ions at the cathode (2) (Margheritini et al., 2020):

$$2H_2O\ (l) \rightarrow O_2\ (g) + 4H^+ + 4e^- \quad (1)$$

$$4H_2O + 4e^- \rightarrow 2H_2\ (g) + 4OH^- \quad (2)$$

This makes the surrounding environment acidic and oxidizing around the anode, alkaline and reducing around the cathode (Medihala et al., 2013). The rise of the local pH, in turn, leads calcium (Ca^{2+}) and magnesium (Mg^{2+}) ions, naturally present in seawater, to react with bicarbonate and hydroxide ions (3) and to precipitate, as shown in the following reactions (Hilbertz and Goreau, 1996):

$$HCO_3^- + OH^- \leftrightarrow CO_3^{2-} + H_2O \quad (3)$$

$$CO_3^{2-} + Ca^{2+} \rightarrow CaCO_3\ (s) \quad (4)$$

$$Mg^{2+} + 2OH^- \rightarrow Mg(OH)_2 \quad (5)$$

This allows the formation of a calcareous scale on the cathode surface (Figure 2, Margheritini et al., 2020), mostly composed of $CaCO_3$ (4) (aragonite) and

$Mg(OH)_2$ (5) (brucite, structurally weaker) in varying proportions (Hunsucker et al., 2021).

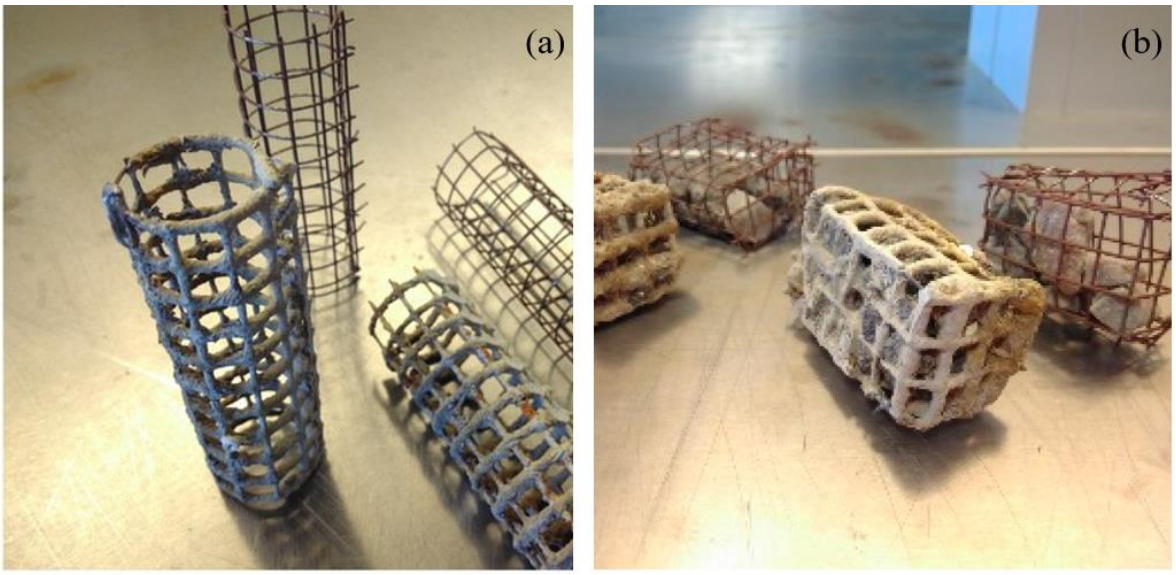

Figure 2. Mineral electrodeposition: (a) wide grid cathode; (b) box with small stones. From Margheritini et al., 2020.

Several factors influence the competition between brucite and aragonite precipitation and calcium/magnesium rate. Brucite is favoured by high voltage and currents resulting in faster mineral precipitation (Goreau and Trench, 2013), at temperatures higher than 30 °C (Karoui et al., 2013), and high pH (>9) (Margheritini et al., 2020). Conversely, aragonite is favoured by slower mineral precipitation on the cathode at temperature of seawater below 7 °C (Goreau and Trench, 2013). In addition, laboratory studies using artificial seawater show that brucite formation is material-dependent (Karoui et al., 2013). At the anode, chloride ions will oxidize and form chlorine gas (Britton and Taylor, 2017):

$2Cl \rightarrow Cl_2 + 2e^-$ (6)

Therefore, applying the mineral accretion technology to the decommissioned oil and gas platforms could be useful for affording protection against corrosion by generating alkaline pH and reducing oxygen diffusion (Margheritini et al., 2020). It is also advantageous because the calcareous layer that precipitates over the platform has the property to be self-repairing and self-attaching as long as the power is supplied to the structure (Little and Wagner, 1995; Goreau and Trench, 2013).

Concerning the benefits for marine life, it has been demonstrated that the material chosen for artificial reefs can influence benthic community development (Salta et al., 2013). For this reason, it is important to choose materials with a structural and chemical composition similar to natural rocks instead of using metals, where the colonization is limited (Siboni et al., 2009). Biorock® technology has been shown to increase the settlement, healing, and growth of marine organisms, even in stressful conditions (Goreau, 2014). When electrically stimulated, reef-building hard corals, gorgonian soft corals, seagrasses, oysters, and salt marsh grasses, typically grow from 2 to 10 times faster and with a mean of more than 3 times greater than in natural conditions (Goreau and Trench, 2013). The rates of coral settlement on electrically charged Biorock® are from 1 to 4 orders of magnitude greater than natural

recruitment (Trench, 2012). In addition, studies demonstrated that broken or damaged corals can completely heal within a day when stimulated by electrical fields, while in natural conditions they can recover within two weeks (Goreau, 2014). Under electrified conditions, clams, tunicates, sponges, and fishes, have been reported to increase their populations (Goreau and Trench, 2013).

Therefore, the reefed platform will inevitably be colonized by different organisms and, by enhancing the structural complexity of the system, will hold higher densities and biomasses of marine flora and fauna (Langhamer, 2012). The composition of fouling communities will depend on environmental parameters, substrate material, and initial bacterial film (Railkin et al., 2004). Indeed, the invertebrate larval settlement could be influenced by the microfouling community composition and successions which are still poorly understood (Zardus et al., 2008).

1.3 Diversity and functions of microbial consortia colonizing different substrates

A newly introduced surface in seawater will immediately undergo physical, chemical, and biological interactions, resulting in changes in its properties (Edyvean et al., 1992). Bacteria are the pioneer colonizers through the formation of a biological film (Edyvean et al., 1992). The biofilm is a syntrophic consortium of microorganisms associated with biotic or abiotic surfaces (Li et al., 2013). It plays an important role in the recruitment of a large number of sessile invertebrates from the surrounding environments (Zardus et al., 2008). In the biofilm, the bacteria are embedded within a slimy, self-produced extracellular matrix, composed of extracellular polymeric substances (EPS) (Skovhus et al., 2017). The EPS matrix consists of DNA, proteins, minerals, polysaccharides, lipids, and water and it is responsible for the further embedding of inorganic particles (Li et al., 2013). The matrix facilitates cell-to-cell communication through signalling molecules, produced by bacteria, which have a fundamental role in controlling biofilm formation and development (Lv et al., 2022). Biofilm formation occurs in different steps, as shown in Figure 3 (Skovhus et al., 2017). It begins when a layer of organic material deposits on a substrate (conditioning film) and promotes the attachment of bacterial cells from the planktonic phase (Li et al., 2013). This

leads to colonization and extensive growth of microorganisms and the formation of a thick biofilm layer (Victoria et al., 2021). Then, the mature biofilm develops; it consists of many different types of microorganisms such as diatoms, benthic dinoflagellates, fungi, and protozoa which follow the colonization after a few days (Antunes et al., 2020).

Its structure is highly heterogeneous in compositions as well as over space and time (Stott and Abdullahi, 2018). The last step is the release of free bacterial cells to the surroundings, able to initiate the cycle again (Victoria et al., 2021).

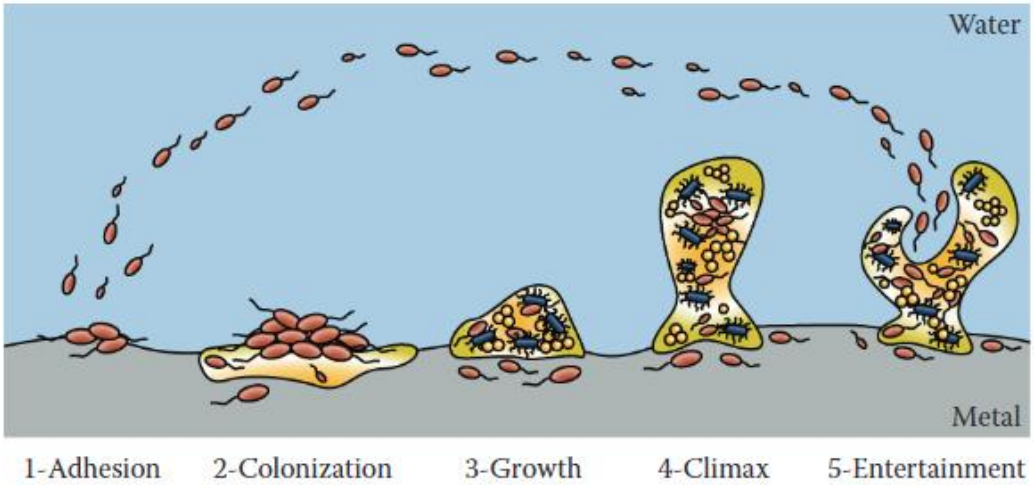

Figure 3. Biofilm development steps. From Skovhus et al., 2017.

Generally, the biofilm adhesion to a metal surface (i.e., unprotected oil and gas platforms) modifies the overall physical and chemical properties of the system, providing conditions that favour the corrosion of the structure (Gu, 2019). Therefore, increasing knowledge on microbial community composition and successions is essential to better understand the mechanisms underlying microbiologically influenced corrosion (Liduino et al., 2021).

1.3.1 *Microbiologically influenced corrosion on unprotected oil and gas platforms*

Oil and gas platforms are often subject to severe corrosion damage that results in decreasing the textile strength, the fracture point, and other mechanical properties, thus leading to a structural failure (Victoria et al., 2021). One of the main causes is microbiologically influenced corrosion (MIC) that results from the presence of microorganisms (bacteria, archaea, fungi, and algae) in biofilms on the metal surface (Skovhus et al., 2017). It is responsible for a global economic loss of 30-50 billion dollars each year, accounting for 20% of the total corrosion losses (Lv et al., 2022). Biofilms can affect corrosion in several ways such as direct effects on cathodic or anodic processes influencing electron movement between the metal and the environment, and changes in oxygen concentration and pH (Gu et al., 2000). In addition, they can cause variations in the surface film resistivity, and generation of metabolic corrosive products (organic acids, sulfuric acids, or reduced sulphur compounds; Gu, 2019). Both the succession of dominant bacteria and the composition of the biofilm have an influence on the corrosion process and the mechanism becomes more complex when many microorganisms exist as a consortium, interacting with each other (Senthilmurugan et al., 2021). The initial oxidation of Fe is driven by dissolved O_2. Subsequent oxidation of Fe^{2+} to Fe^{3+} is carried out by the iron-oxidizing bacteria which, in the early biofilm formation stages, grow rapidly and provide

a suitable microenvironment for anaerobic sulfate-reducing bacteria (SRB) to proliferate (Wang et al., 2014). SRB are the most common MIC causing microorganisms in a mixed biofilm where they occupy the lowest levels, closer to the metal surface (low oxygen concentration) (Victoria et al., 2021; Figure 4, Stott and Abdullahi, 2018).

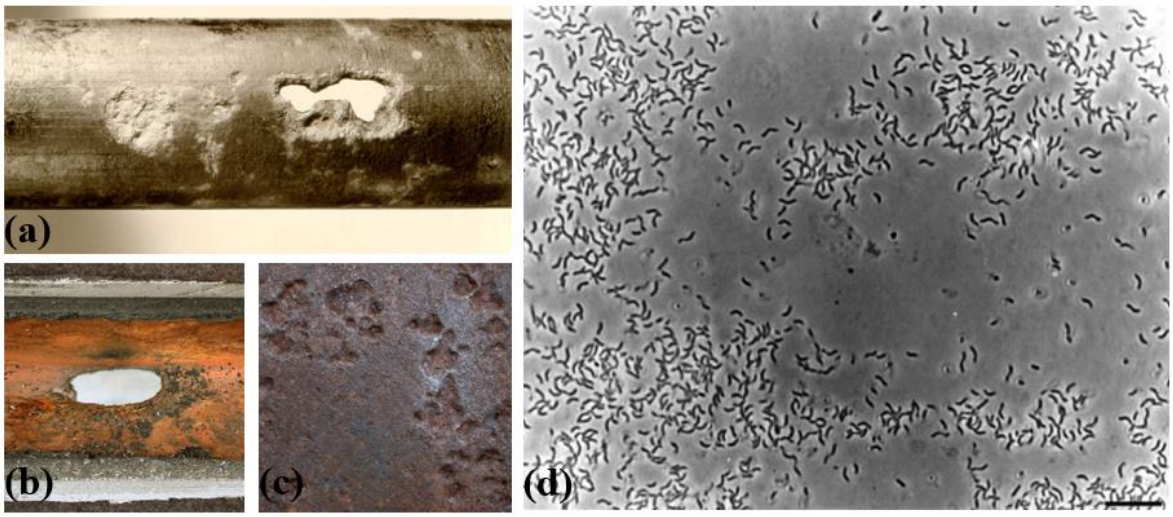

Figure 4. (a), (b), (c) Typical morphology of SRB-mediated MIC; (d) *Desulfovibrio*, a common genus of SRB, bar = 10 μm in length. From Stott and Abdullahi, 2018.

SRB are anaerobic, chemolithotrophic bacteria, which use sulfate as an electron acceptor thus generating sulfide (e.g., H_2S) (Zhou et al., 2021). Hydrogen sulfide is a highly corrosive compound and can react with metal surfaces forming precipitates of the black iron sulfide (FeS) (Stott and Abdullahi, 2018). In presence of oxygen, the oxidation of FeS produces the highly corrosive elemental sulfur (S_0) (Skovhus et al., 2017). Manganese- and iron-oxidizing bacteria, which obtain energy from the oxidation of these metals, are often

found associated with SRB (Skovhus et al., 2017). They form deposits of oxides and hydroxides over the metal surface and provide oxygen-depleted zones for the SRB to proliferate (Sachan and Singh, 2020). Other bacteria usually associated with SRB are the sulfur-oxidizing bacteria (SOB); they are aerobic chemolithotrophic microorganisms that oxidize reduced forms of inorganic sulfur compounds to sulfuric acids thus resulting in an intense acidic zone (Stott and Abdullahi, 2018; Gu, 2019). Other microorganisms responsible for corrosion are the acid-producing bacteria (APB) which carry out the anaerobic fermentation that converts carbohydrates to weak organic acids (e.g., acetic, lactic, formic, butyric acids) and CO_2 (Lin and Ballim, 2012).

Even though damages caused by fungal activity are less prevalent than those of bacteria, fungal-influenced corrosion can have relevant implications (Little and Ray, 2002). Fungi are aerobic eukaryotic organisms with a heterotrophic metabolism (Victoria et al., 2021). They derive their energy by degrading organic sources and generating organic acids. This leads to a drop in the pH of the surrounding water and under the microbial mat, responsible for direct acid corrosion (Little and Ray, 2002). They are also capable of generating corrosive oxidants (e.g., hydrogen peroxide; Gu, 2019).

Overall, the activities of these MIC-causing associations have been mainly reported to occur on metal structures leading to the production of an extensive

corrosion film (Little and Wagner, 1995). This can be avoided by applying Cathodic Protection which is the most widely used technique to prevent corrosion film formation on submerged structures (Liduino et al., 2021). This practice influences the growth and activities of microbial communities and imposes selective pressures on certain microbial groups (Torsvik et al., 2002).

1.3.2 Interactions between microbial communities and electric current application

In seawater, during the application of cathodic protection, the formation of a calcareous layer on the metal surface occurs (Margheritini et al., 2020). In a biologically active medium, interactions take place between the biofilm, the calcareous deposits, and the metal surface (Edyvean et al., 1992). The shifts in pH and redox conditions of the environment after the application of the impressed current together with the calcareous substrate composition influence the biofilm formation and the development of the macrofouling community (Siboni et al., 2009). On the other hand, biological activity can interfere with cathodic protection inducing changes in the current demand (Hernandez et al., 1992). Microbial communities can either be inhibited or stimulated by the application of an electric current (Medihala et al., 2013). Different studies have demonstrated a very strong initial inhibitory effect of CP on the settlement and reproduction of bacteria during the early stages of exposure (e.g., hours or days)

(Sultana et al., 2015). Conversely, over a relatively long time scale (e.g., weeks) significant microfouling activity, during calcareous scale deposition, has been shown, particularly when the scale builds up and provides a barrier film, leading also to the settlement of macrofouling organisms (Edyvean, 1984). The initial application of cathodic protection decreases the number of bacteria settling compared to unprotected conditions (Hernandez et al., 1992). The degree of this reduction is dependent on current flow and electric potential (Edyvean et al., 1992). Ulanovski and Ledenev (1981) demonstrated that CP, in presence of SRB, decreased corrosion by a factor of 8 or 9. The CP is enhanced at more negative potentials (required to counteract SRB activity) and seems to be also temperature-dependent (more pronounced effects at 12°C compared to 20°C) (Edyvean et al., 1992; de Gómez Saravia et al., 1997).

The inhibitory effect on the bacterial settlement is likely due to the bacterial release of negatively charged glycocalyx which is electrostatically repelled from the cathodic surface (Sultana et al., 2015). Furthermore, the alkaline pH generated at the cathodic surface could reduce bacterial adherence (Edyvean et al., 1992).

Despite the overwhelming evidence that bacteria can colonize calcareous deposits on cathodically protected surfaces, information about their interactions is still limited (Liduino et al., 2021).

Siboni et al. (2009) demonstrated a dynamic succession of the biofilm on a metallic net covered with $CaCO_3$ even after disconnection from electric current. After 72h from disconnection, Alpha- and Gammaproteobacteria were identified as early colonizers taxa, while after two weeks, an increase of sequences related to Actinobacteria demonstrated a changing succession (Siboni et al., 2009). Medihala et al. (2013), found that the biofilm was significantly thicker on electrified structures compared to that on not electrified ones. They observed that the community composition was markedly different between protected and unprotected structures and between biofilm and water samples.

Despite cathodic protection has been studied for decades, findings from different experiments are hard to compare because of variations in currents and potentials applied and because of the diverse physicochemical settings displayed by different marine environments (Istanbullu et al., 2012; Siboni et al., 2009). Therefore, investigations on shifts of microbial assemblages of the biofilm collected from protected and unprotected metal surfaces and from surrounding seawaters can be relevant for better understanding the biological processes prompted by the mineral accretion technology applied to offshore oil and gas platforms.

2. AIMS

The aim of this thesis is to investigate microbial assemblages associated with prototypes of offshore oil and gas platforms using both traditional (stereo-light, epifluorescence microscopy) and metabarcoding analyses (targeting the 16S and Internal Transcribed Spacer 2 ribosomal RNA genes). In particular, the objectives of this study are:

- comparing prokaryotic abundance and diversity of the biofilm deposited on electrified and on not electrified structures;
- analysing the assemblage composition of fungi and their successions;
- understanding the dynamics of the biofilm formation through comparative analyses between seawater and microbial biofilm.

This investigation can shed light on the interactions between microbial biofilm and artificial submerged substrates of offshore oil platforms, expanding our knowledge of the potential future applications of the decommissioned plant reuse.

3. MATERIALS AND METHODS

3.1. Study area and sample collection

This experiment was conducted in the framework of the PLaCE project that aims to test the efficiency of mineral accretion technology. It employs specially designed artificial steel structures, prototypes of those that will be installed around the platform Viviana, in the Abruzzo region, Adriatic Sea. The structures were installed in July 2020 in zone A of Bergeggi Island MPA (SV), Ligurian Sea, at 21.7 m depth (44°14'05,94" N; 8°26'46" E), Figure 5.

Figure 5. Zonation of Bergeggi MPA and location of the metal structures.

The structures consisted of two modules composed by 8 cathodes in the shape of cylindrical bars (steel tubes, diameter 1 inch, and length 90 cm) as shown in Figure 6.

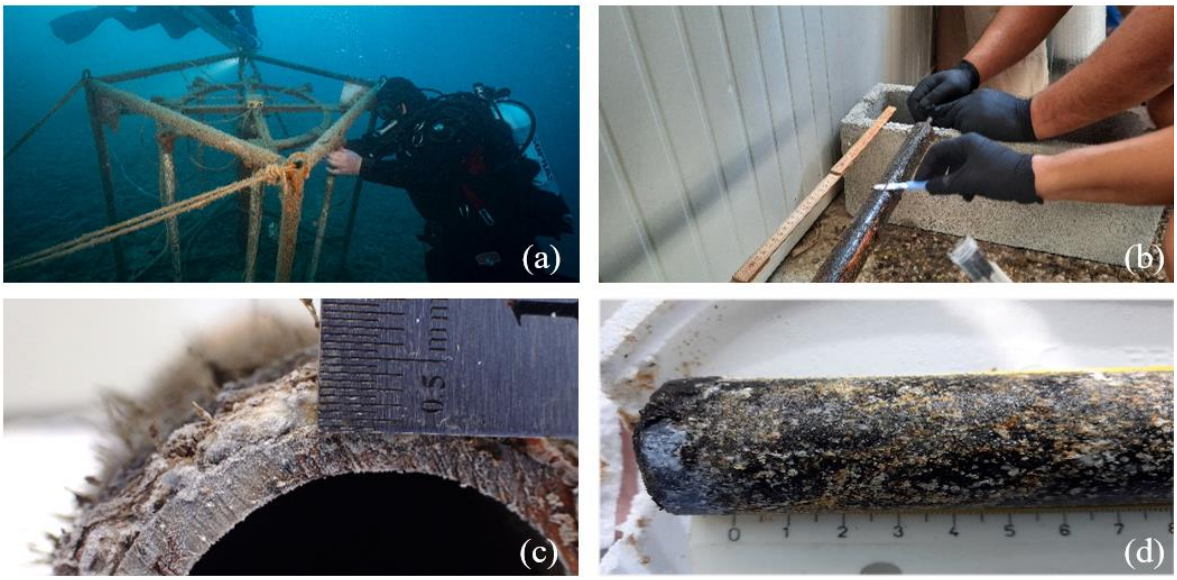

Figure 6. (a) Removal of the bars during scuba diving; (b) Scraping for biofilm sampling; (c),(d) Initial mineral deposition on electrified bars.

One of the two modules was electrified and contained a not removable central titanium anode, while the second, not electrified, was used as a control. The electrified structure was powered by extra low voltage DC current (2.5 volts). Each of the bars was collected at different times: 31st July 2020, 5th September 2020, 24th October 2020, 16th January 2021, and 24th April 2021(the last sampling was performed after electric disconnection). Biofilm samples were taken from both sides of the bars through "scraping" by means of sterile scalpels and collected into 50-ml falcon tubes. In addition, seawater samples (5 litres) from the area in front of the two structures were collected in sterile tanks. Biofilm and water samples were immediately frozen at -20°C for downstream molecular analyses. A multi-parametric probe (Micro CAT C-T-(P)-ODO

Recorder) for the collection of environmental data (conductivity, temperature, and dissolved oxygen) was employed.

3.2 Prokaryotic abundance and biomass

Total prokaryotic cell counts were performed using the SYBR Green I direct count procedure (Danovaro, 2010). Briefly, the biofilm samples (on average 0.08 g of dry weight) were sonicated (Branson Sonifier 2200, 60W) 3 times for 1 minute after the addition of 0.2 μm pre-filtered and autoclaved seawater and 0.2 μm pre-filtered tetrasodium pyrophosphate solution (final concentration, 5 mM). Specimens were then incubated for 15 min in the dark at room temperature and properly diluted with 0.2 μm pre-filtered and autoclaved seawater. Then, seawater and biofilm samples were filtered onto 0.2 μm pore-size Nuclepore black filters, diameter 25 mm (Whatman®) and then stained with 40μl of SYBR Green I (10000× stock) diluted 1:40 with sterile Milli-Q® water. Filters were incubated in the dark for 20 min, rinsed three times with 3 ml of 0.02-μm pre-filtered Milli-Q® water, and then mounted onto microscope slides by using 20 μl of antifade solution (50% phosphate-buffered saline, pH 7.4, 50% Glycerol, and 0.5% ascorbic acid). At least 20 optical fields and 200 cells per filter were counted randomly using epifluorescence microscopy under blue light (x100 oil-immersion objective). For the determination of the

prokaryotic biomass, prokaryotic cell size was converted into bio-volume following inter-calibration with Scanning Electron Microscope (SEM) based size determinations and converted into carbon content assuming 310 fgC μm^{-3} (Danovaro, 2010). This is in line with previous studies and thus enables comparisons between biofilm and available data for the deep seafloor (Danovaro et al., 2016; Rastelli et al., 2016). Data of prokaryotic abundance and biomass for biofilm samples were expressed as number of cells and μg C per gram of dry weight biofilm, respectively. For seawater samples as number of cells and μg C per ml of seawater.

3.3 Seawater and biofilm DNA extraction

One L aliquots of seawater collected in July, September, October, January, and April were vacuum-filtered through 0.2 μm pore-size Nuclepore white filters, diameter 47 mm (Whatman®) (n =2 filters per sample) and stored in 15 ml sterile transport tubes at –20 °C until DNA extraction.

Total genomic DNA was extracted from filters using the PowerSoil DNA Isolation Kit (MOBIO Laboratories Inc.; Qiagen, Hilden, Germany) following the manufacturer's instructions. DNA extraction and purification were carried out in two replicates for each seawater sample (n=2).

DNA extractions of biofilm samples collected from electrified and not electrified bars in July, September, October, January, and April were carried out in two replicates for each sample (n=2) using the same kit employed for seawater.

All DNA extracts were stored at − 20 °C. DNA quantification and quality analyses were performed with a NanoDrop 1000 Spectrophotometer using 1.5 µl of DNA for each sample to ascertain the suitability of DNA samples for further analysis.

3.4 Amplification and sequencing of 16S and Internal Transcribed Spacer 2 (ITS2) ribosomal RNA genes

For the analysis of prokaryotic diversity, the V4-V5 hypervariable region of the 16S rRNA gene was amplified using the primer set 515F-Y (5′-GTGYCAGCMGCCGCGGTAA-3') and 926R (5′-CCGYCAATTYMTTTRAGTTT-3') (Parada et al., 2016) following the Illumina protocol. Amplification reactions consisted of 18 µl of 0.02 µm filtered (Whatman®, Anotop®, Merck KGaA, Darmstadt, Germany) and sterile Milli-Q® water, 5 µl of 5x My Taq Reaction Buffer (Bioline), 0.25 µl of each primer (20 µM), 0.5 µl of My Taq™ HS DNA Polymerase (5 U/µl concentration), and 1 µl of DNA extracted. Negative (0.02 µm pre-filtered and

autoclaved Milli-Q® water) and positive controls (extracted and purified genomic DNA of *Escherichia coli*) were used.

The thermal cycling profile consisted in 3 min at 95°C, followed by 35 cycles of 45 s at 95°C, 45 s at 50°C, 1 min and 30 s at 68°C, with a final extension of 5 min at 68°C.

For fungal diversity analysis, the ITS2 region of the Internal Transcribed Spacer (ITS), was amplified using the primer set ITS3f (5′-GCATCGATGAAGAACGCAGC-3′) and ITS4r (5′-TCCTCCGCTTATTGATATGC-3′) (White et al., 1990).

The reaction mixture consisted of 16.5 µl of 0.02 µm filtered (Whatman®, Anotop®, Merck KGaA, Darmstadt, Germany) and sterile Milli-Q® water, 5 µl of 5x My Taq Reaction Buffer (Bioline), 1 µl of each primer (10 µM), 0.5 µl of My Taq™ HS DNA Polymerase (5 U/µl concentration), and 1 µl of DNA extracted. Negative (0.02 µm pre-filtered and autoclaved MQ water) and positive controls (extracted and purified genomic DNA of *Saccharomyces cerevisiae*) were used.

The thermal cycling profile consisted in 5 min at 95°C, followed by 32 cycles of 40 s at 94°C, 40 s at 55°C, 1 min at 72°C, with a final extension of 7 min at 72°C.

Successful DNA amplifications were verified by 1.5% agarose gel electrophoresis (80V, 1 h) stained with GelRed™ (2x) in 1x TAE Buffer (40 mM Tris-acetate and 1 mM EDTA, pH 8.3) (Russell and Sambrook, 2001). Different DNA dilutions were tested to exclude potential PCR bias due to the presence of inhibitors.

Aliquots of the extracted DNA from biofilm and seawater samples were sent to Genomix4Life laboratories (www.genomix4life.com) for amplicon library preparations and sequencing. Illumina sequencing MiSeq 2 x 300bp of 16S and ITS2 amplicon libraries were carried out on two different runs with an output of 20M reads for each run.

3.5 16S and ITS2 Amplicon sequences analysis

For bacterial diversity, raw sequences were analysed using the QIIME2 pipeline (Callahan et al., 2016; Bolyen et al., 2019). First, pair-end reads were trimmed for barcode and primer sequences using CUTADAPT (Martin et al., 2011). Demultiplexed sequences were denoised into amplicon sequence variants (ASVs) through DADA2 pipeline (Callahan et al., 2016). This method filtered out noisy sequences, corrected errors in marginal ones, removed chimeric sequences and singletons, joined denoised paired-end reads, and dereplicated those sequences. Resulting ASVs of each sample were normalized

to the least number of sequences reaching saturation (5500) to allow comparison among samples with different reads abundance (Hughes and Hellmann, 2005).

A subset of the SILVA database (release 138) (Quast et al., 2012) was created through the extract-reads procedure within QIIME2: database sequences were trimmed to the region amplified by the primers used; sequences from the subsetted database were then used as an input for subsequent classification steps carried out on the representative sequences using the *classify-consensus-vsearch* tool within QIIME2, with default parameters (Rognes et al., 2016). ASVs were aligned and the alignment was used to create a rooted tree within QIIME2 using the implemented MAFFT and FastTree tools (Price et al., 2010). For fungal diversity, paired-end sequences were analysed within the QIIME2 environment (Callahan et al., 2016; Bolyen et al., 2019). First, the ITSxpress plugin was used to trim sequences targeting the ITS2 region (Rivers et al., 2018). Then, trimmed paired-end sequences were analysed through the DADA2 procedure (Callahan et al., 2016), and the resulting biologically significant Amplicon Sequence Variants (ASVs) were compared against the UNITE database (Version: 8.3; Last updated: 2020-12-11) for taxonomic affiliation (Nilsson et al., 2019). Taxonomic affiliation was performed through the USEARCH SINTAX procedure (Edgar et al., 2018) using default

parameters. To allow a proper comparison among samples, the ASV table was then rarefied to 1200 randomly-selected sequences, corresponding to the lowest read count obtained in our samples (Hughes and Hellmann, 2005; Gihring et al., 2012). Samples with very low read counts were not included in downstream analyses.

3.6 Bioinformatic analysis of metabarcoding data

For both bacterial and fungal diversity, the following informatic elaborations were applied. In particular, total ASVs richness, alpha-diversity analysis, and taxonomic composition were performed using R4.0.3 through Phyloseq, Microbiome, and Vegan packages (McMurdie and Holmes, 2013; Lahti and Shetty, 2017; Oksanen et al., 2020). The same packages were applied for the Principal Coordinates Analysis (PCoA) ordination based on Bray-Curtis dissimilarity that was used to visualize the dispersion of microbial community among samples. Then, a hierarchical clustering dendrogram of the total ASVs based on Bray-Curtis distance matrix was built. A heatmap was constructed using Pheatmap package to better visualize and facilitate data analysis (Kolde, 2019). Relative abundance values were expressed as CLR-transformed values; samples and taxa were clustered with the ward.D2 method. Finally, Venn diagrams showing exact numbers of shared and exclusive ASVs between

samples were constructed using the MicEco and Eulerr packages (Russel, 2020; Larsson, 2018).

4. RESULTS

4.1 Environmental parameters

Environmental data (conductivity, temperature, and dissolved oxygen) collected in different months in the surrounding waters of the structures are reported in Table 1. Seawater in January, compared to the other months, was characterized by the lowest temperature (14.68 °C) and the highest dissolved oxygen (6.10 mg/L). Salinity did not reveal remarkable changes (ranging from 38.05 and 37.80).

Month	T	DO	S
July	19.87	5.44	38.05
September	21.66	5.15	38.01
October	21.13	5.02	37.89
January	14.68	6.10	37.80

Table 1. Environmental parameters collected by the multi-parametric probe in the different months: temperature (T), dissolved oxygen (DO), and salinity (S). Temperature is expressed in °C, dissolved oxygen in mg/L.

4.2 Chemical and mineralogical characterization

Deposits on electrified bars (Table 2) showed the highest growth rate in September (72.94 μm d^{-1}) in correspondence of the highest current regime (0.594 A). The percentage of deposited aragonite was inversely related to the deposit thickness. Brucite began to be produced after July and maintained a nearly constant percentage (between 55% and 57% in the following months).

The same pattern can be found in the percentage of Mg, a constituent of brucite, whereas a decreasing temporal pattern can be found in the percentage of Ca.

Month	C	DT	GR	%A	%B	%Mg	%Ca	%Fe
July	0.132	0.238	21.42	95.8	0.1	3.5	53.1	12.5
September	0.594	1.274	72.94	44.0	56.0	47.8	41.5	4.6
October	0.258	1.618	17.02	42.5	57.0	50.1	40.7	3.1
January	0.108	2.390	10.38	42.2	55.0	46.4	39.7	6.1
April				43.0	57.0	45.7	38.4	7.1

Table 2. Electric variables and mineralogical analyses of the deposits on electrified bars. Current (C) is expressed in Ampere, deposit thickness (DT) in mm, growth rate (GR) in $\mu m\ d^{-1}$. %A is the percentage of aragonite, %B is the percentage of brucite.

XRF and XRD analyses of not electrified bars (Table 3) revealed an initial high percentage of lepidocrocite (92%), a reddish iron oxide-hydroxide mineral, generally present in the rust scale. On the contrary, maghemite, a member of the family of iron oxides, showed the highest percentages in October (72.1%) and was absent in the first month of monitoring. Percentages of Mg and Ca showed both an increasing trend over time whereas the percentage of Fe showed a decreasing trend over time.

Month	%L	%M	%Mg	%Ca	%Fe
July	92.0	0.0	0.0	1.7	92.2
September	58.1	30.8	0.9	1.3	88.3
October	23.5	72.1	2.2	5.0	81.9
January	28.6	59.3	2.8	7.6	74.2
April	43.3	23.6	5.7	15.6	63.7

Table 3. Mineralogical analyses of not electrified bars. %L is the percentage of lepidocrocite, %M is the percentage of maghemite.

4.3 Prokaryotic abundance and biomass in biofilm and seawater samples

Prokaryotic abundances in biofilm samples (Figure 7a) showed temporal changes at the different months. Electrified and not electrified bars were characterized by a similar pattern, with the highest values reached in September (ranging from 9.4×10^8 to 2.0×10^9 cells g^{-1}). Differences can be observed in January between not electrified and electrified bars, the latter showing higher values (ranging from 6.5×10^8 to 1.7×10^9 cells g^{-1}) than not electrified bars (ranging from 8.2×10^7 to 2.2×10^8 cells g^{-1}).

Prokaryotic biomass of biofilm samples (Figure 7b) followed a similar pattern, with higher values reached in September (ranging from 20.44 to 39.65 μgC g^{-1}). Differences can be observed in January between not electrified and

electrified bars, the latter showing higher values (ranging from 8.97 to 25.33 µgC g^{-1}) than not electrified bars (ranging from 0.99 to 2.51 µgC g^{-1}).

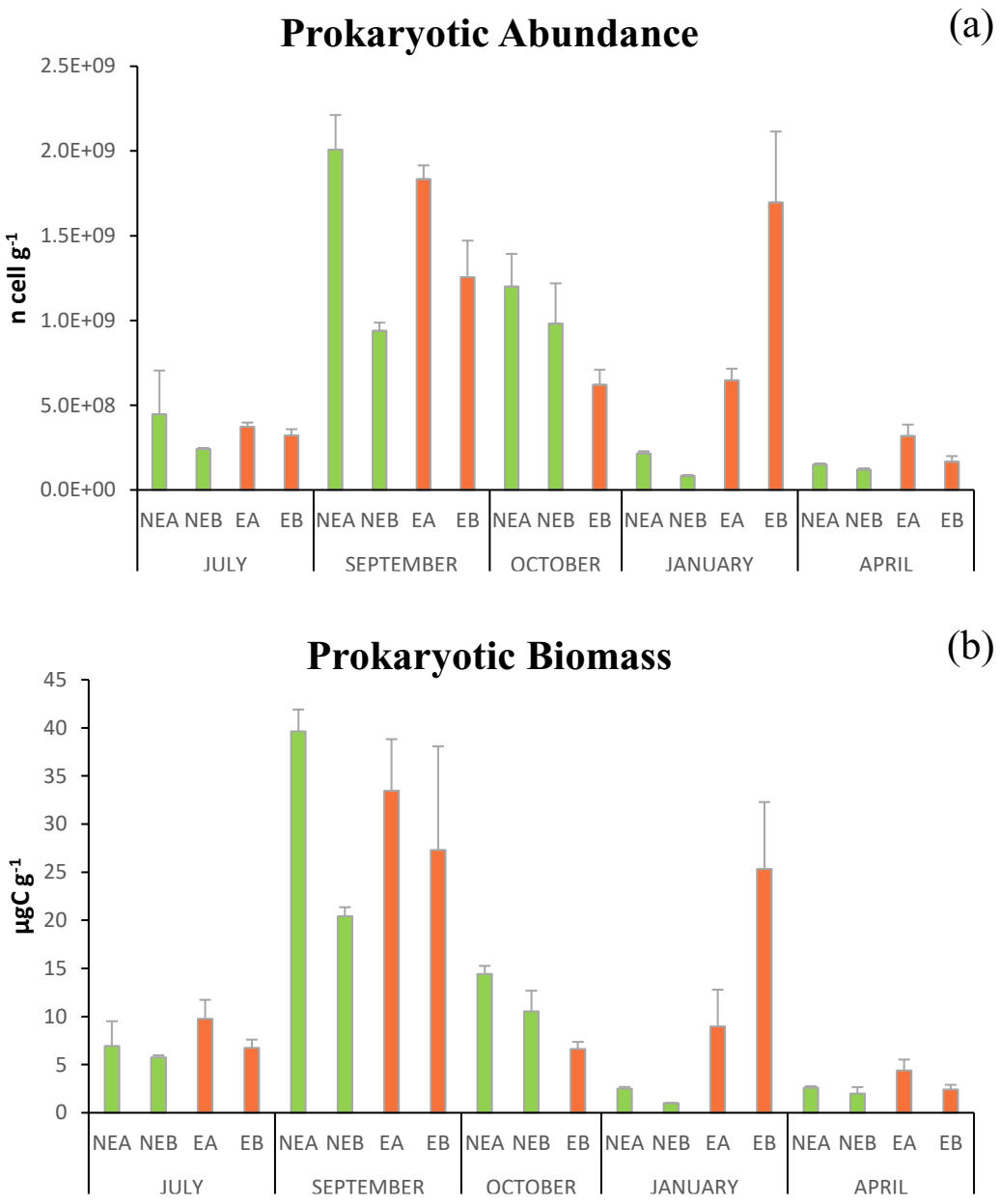

Figure 7. Prokaryotic abundance (a) and prokaryotic biomass (b) of biofilm samples at different moths (July, September, October, January, April) from electrified (in orange) and not electrified (in green) bars. Data are expressed as number of cells per gram (dry weight) of biofilm for prokaryotic abundance and in µgC per gram (dry weight) of biofilm for prokaryotic biomass.

Prokaryotic abundances of seawater samples (Figure 8a) showed temporal changes over the different months. The highest value ($2.1 \times 10^5 \pm 1.2 \times 10^4$ cells ml^{-1}) was reached in September.

Prokaryotic biomass of seawater samples (Figure 8b) followed a similar pattern, with the highest value reached in September as well ($2.3 \times 10^{-3} \pm 4.5 \times 10^{-6}$ µgC ml^{-1}).

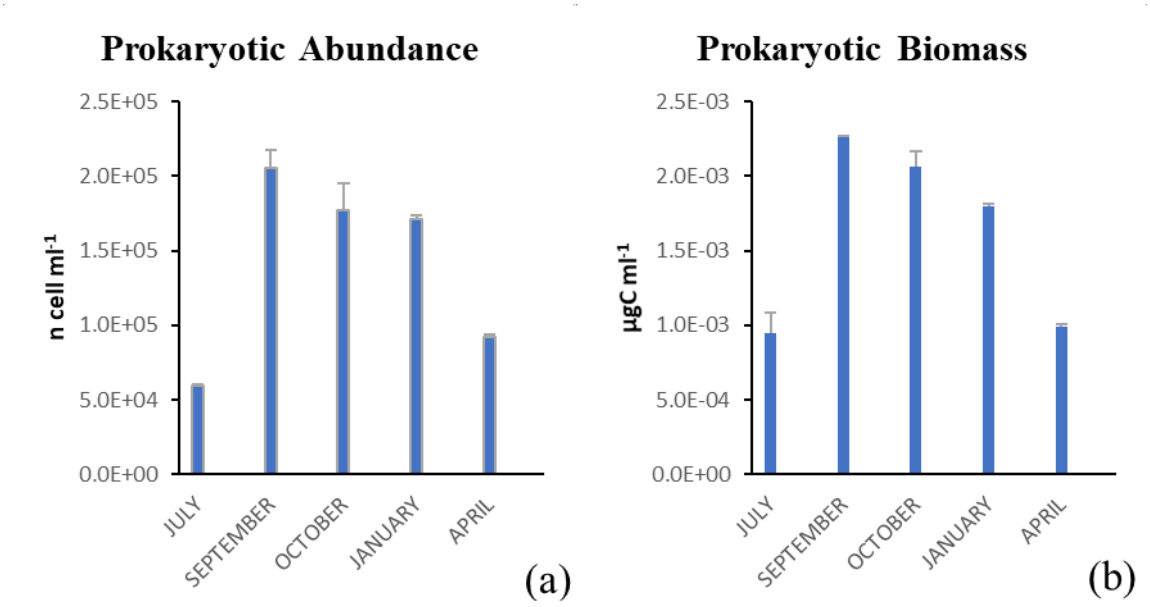

Figure 8. Prokaryotic abundance (a) and prokaryotic biomass (b) of seawater samples at different moths (July, September, October, January, April). Data are expressed as number of cells per ml of seawater for prokaryotic abundance and in µgC per ml of seawater for prokaryotic biomass.

4.4 Alpha and Beta diversity analysis of prokaryotic assemblages

4.4.1 Total ASVs richness

After initial quality filtering and chimera removal, from 5507 to 220201 high-quality sequences were collected from each sample and denoised forming a

total of 32214 amplicon sequence variants (ASVs); the total ASVs richness was then calculated from each sample (Figure 9).

Total ASVs richness was higher among biofilm samples than among seawater samples, ranging from 480.5 ± 117.3 ASVs to 1095.3 ± 742.6 ASVs and from 304 ± 43.4 ASVs to 710.5 ± 159.6 ASVs, respectively.

Biofilm samples of electrified and not electrified bars showed higher richness in April (1095.3 ± 742.6 ASVs and 1035.8 ± 69.1 ASVs, respectively) than in all the other months (ranging from 480.5 ± 117.3 ASVs to 871.5 ± 43.7 ASVs). The lowest richness was found in January in the samples of both electrified and not electrified bars (480.5 ± 117.3 ASVs and 595.5 ± 128.4 ASVs, respectively).

Seawater samples, as well, showed higher richness in April (710.5 ± 159.6 ASVs) than in all the other months (ranging from 304 ± 43.4 ASVs to 572.5 ±150.4 ASVs). The lowest richness was found in September.

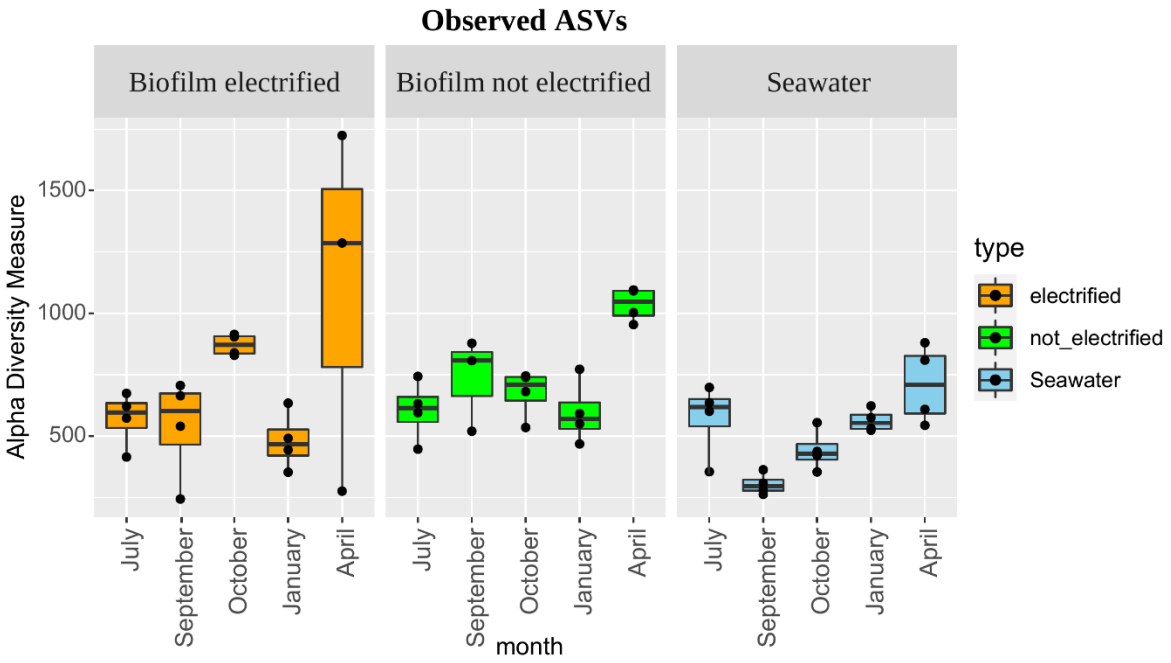

Figure 9. Estimated number of ASVs for each sample.

Differences within the ASVs richness between biofilm and seawater samples were supported by rarefaction curve analyses (Figure 10).

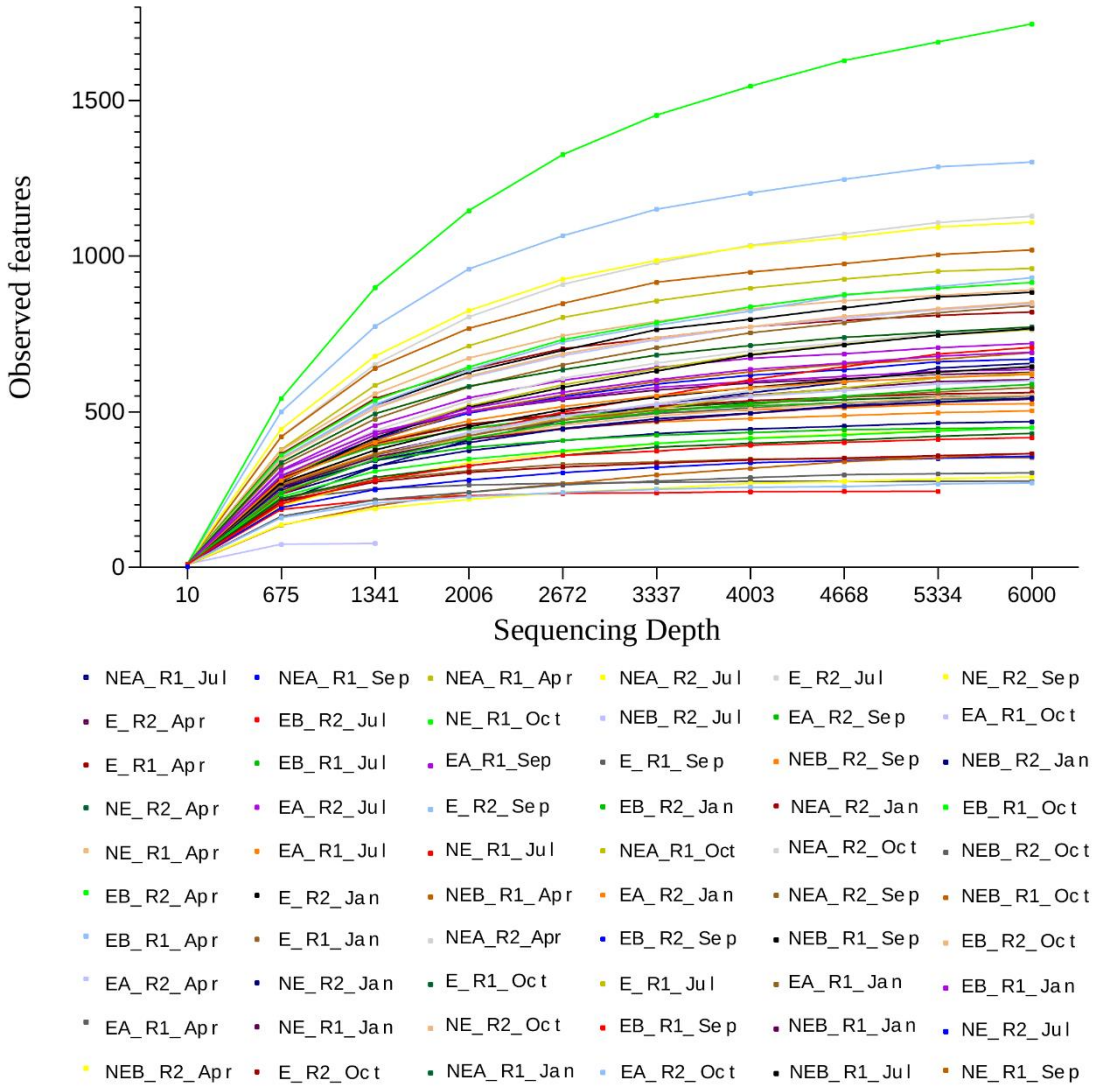

Figure 10. Rarefaction curve of observed ASVs in biofilm and seawater samples.

4.4.2 Alpha diversity indices

Diversity measures for biofilm and seawater ASVs produced different Shannon (H'), Pielou's (J), and Simpson (S) indices, as reported in Table 4 and Figure 11. Shannon diversity was similar between biofilm and seawater samples (H' ranging from 4.18 ± 0.41 to 6.50 ± 1).

Biofilm samples of electrified and not electrified bars showed similar patterns with higher diversity in April (H'= 6.50 ± 1 and H'= 6.35 ± 0.25, respectively) compared to the other months (H' ranging from 4.87 ± 0.47 to 6.05 ± 0.06). In the seawater samples, as well, the highest diversity was found in April (H'= 5.86 ± 0.31) and the lowest one in September (H'= 4.18 ± 0.41) compared to the other months (H' ranging from 5.06 ± 0.20 to 5.46 ± 0.08).

The evenness index was similar between biofilm and seawater samples (J ranging from 0.73 ± 0.08 to 0.96 ± 0.01). No significant differences were found among biofilm samples in relation to the electrification state. Biofilm samples of electrified and not electrified bars showed the highest evenness indices in April (J = 0.96 ± 0.01and J = 0.92 ± 0.03, respectively) compared to the other months (J ranging from 0.76 ± 0.06 to 0.89 ± 0.01). For seawater samples, as well, the highest evenness index was found in April (J = 0.90 ± 0.02) and the lowest in September (J = 0.73 ± 0.08) compared to the other months (J ranging from 0.80 ± 0.01 to 0.86).

Simpson index did not show significant differences between biofilm and seawater samples (S ranging from 0.95 ± 0.04 to 1). The lowest Simpson index was found in seawater samples of September (S = 0.95 ± 0.04) and the highest was found in electrified bars of biofilm samples of April (S = 1).

	Biofilm Electrified			Biofilm Not Electrified			Seawater		
Month	H’	J	S	H’	J	S	H’	J	S
July	5.25 ±0.34	0.83 ±0.03	0.99 ±0.01	4.87 ±0.47	0.76 ±0.06	0.97 ±0.02	5.06 ±0.20	0.80 ±0.01	0.98 ±0.00
September	5.47 ±0.37	0.88 ±0.02	0.99 ±0.00	5.83 ±0.22	0.89 ±0.00	0.99 ±0.00	4.18 ±0.41	0.73 ±0.08	0.95 ±0.04
October	6.05 ±0.06	0.89 ±0.01	0.99 ±0.00	5.29 ±0.12	0.81 ±0.02	0.98 ±0.00	5.14 ±0.15	0.85 ±0.01	0.99 ±0.00
January	5.30 ±0.37	0.86 ±0.03	0.98 ±0.01	5.31 ±0.55	0.83 ±0.07	0.97 ±0.02	5.46 ±0.08	0.86 ±0.00	0.99 ±0.00
April	6.50 ±1	0.96 ±0.01	1 ±0.00	6.35 ±0.25	0.92 ±0.03	0.99 ±0.00	5.86 ±0.31	0.90 ±0.02	0.99 ±0.00

Table 4. Diversity indices used in this study. H', Shannon index; J, Pielou's index; S, Simpson index.

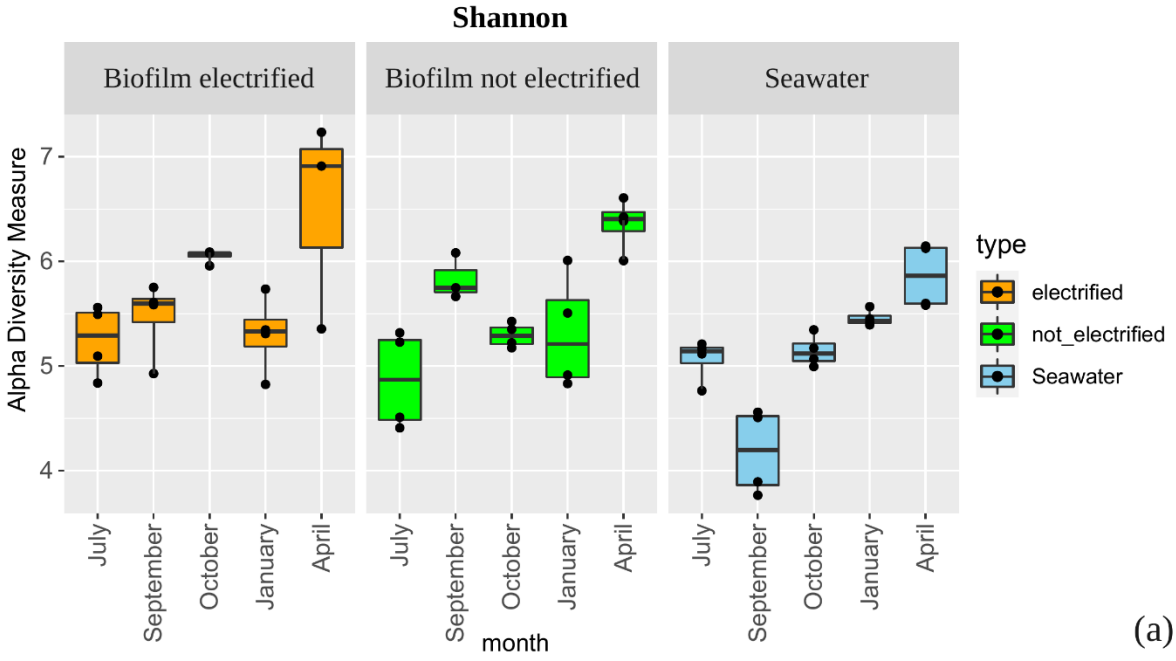

(a)

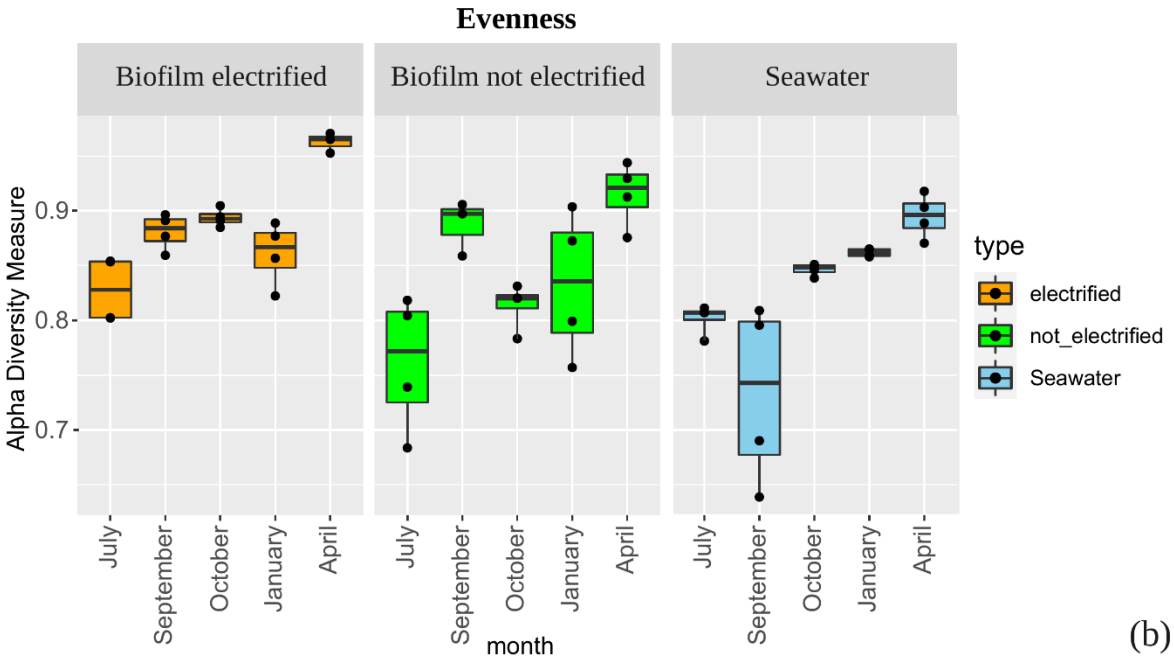

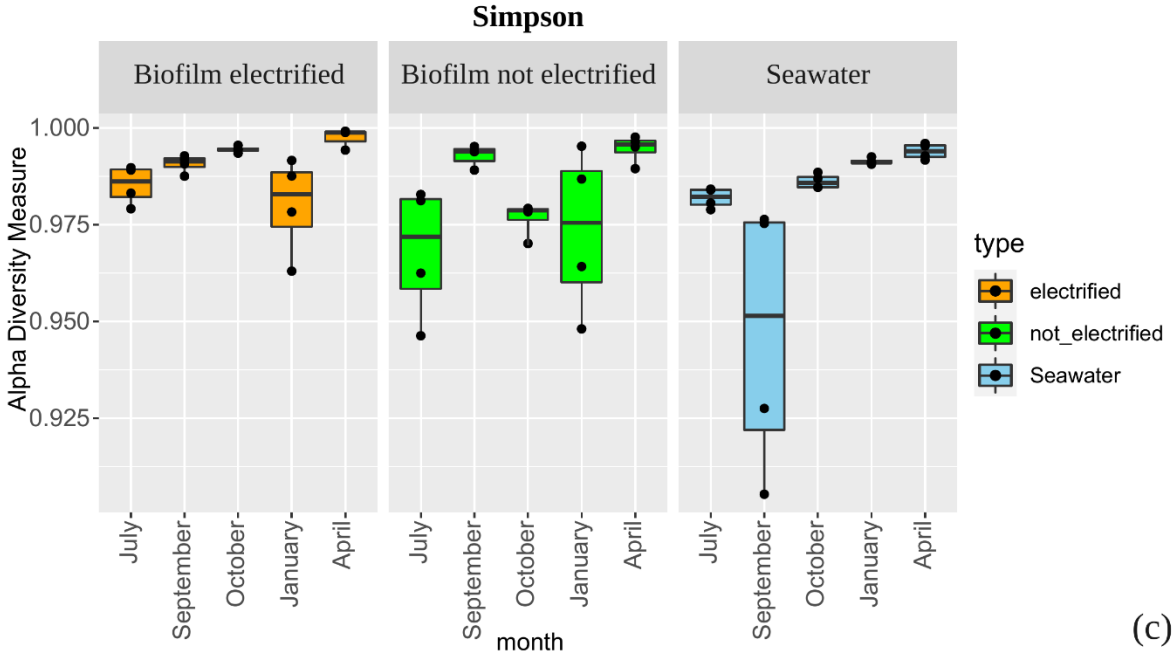

Figure 11. Shannon (a), Pielou's (b), and Simpson (c) indices.

4.4.3 Beta diversity analysis

Principal coordinates analysis (PCoA) ordination, based on Bray-Curtis dissimilarity, graphically represented the resemblance matrix among all samples analysed (Figure 12). Seawater and biofilm displayed dissimilar prokaryotic assemblages, with a clear clustering pattern of samples collected in April (Figure 12a). PCoA of biofilm showed a clustering pattern between the different months. In addition, every month displayed a grouping pattern between samples collected from biofilm of electrified and not electrified bars (Figure 12b).

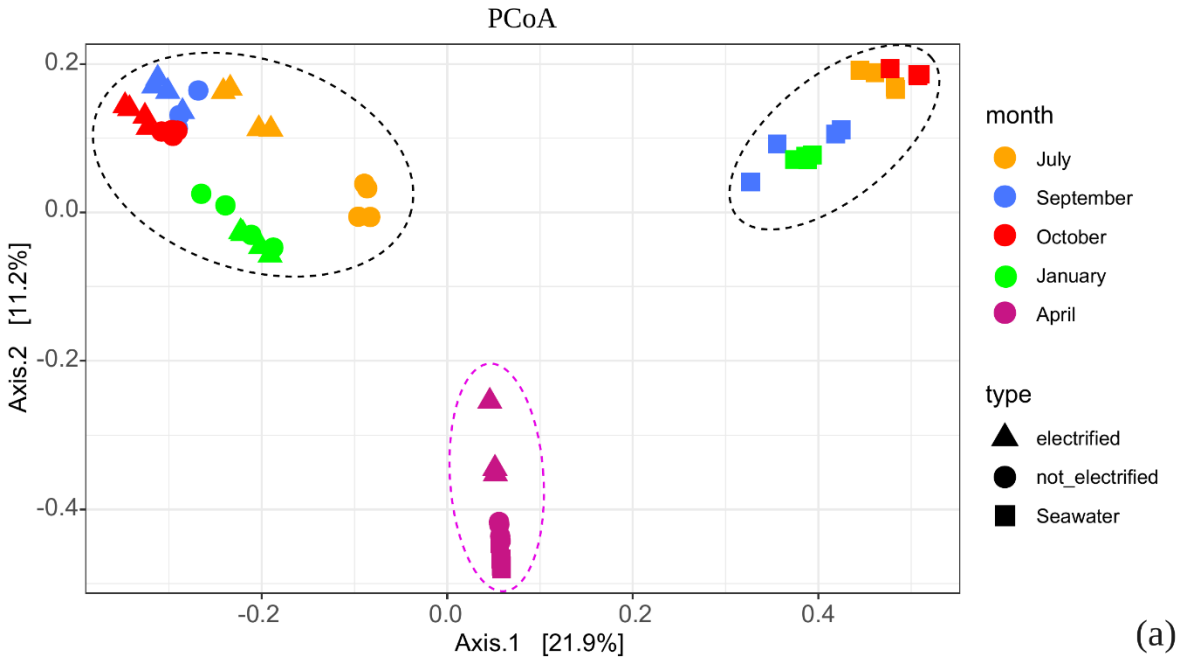

(a)

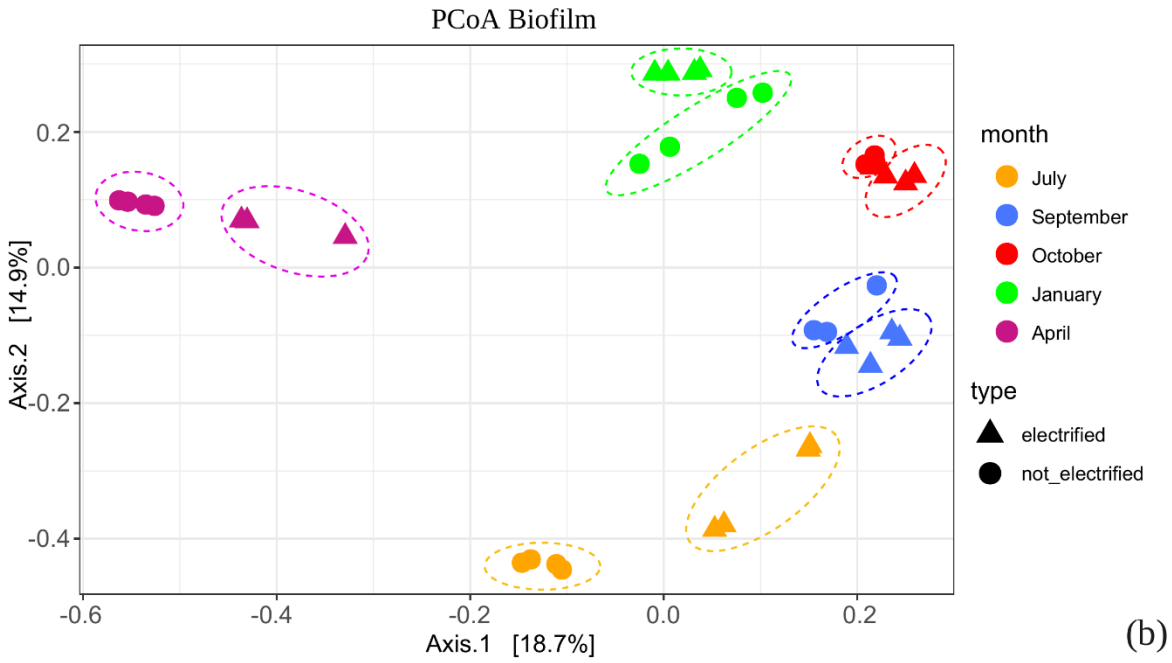

Figure 12. Principal coordinate analysis (PCoA) based on Bray-Curtis dissimilarity matrix of prokaryotic communities associated with seawater and biofilm samples (a) and with biofilm samples (b) collected in different months: July, September, October, January, April.

The results were further validated by the construction of a hierarchical clustering dendrogram of the total ASVs, based on the Bray-Curtis distance matrix (Figure 13). The dendrogram showed a clear clustering pattern of biofilm, seawater, and April month (which showed 100% dissimilarity with the other months).

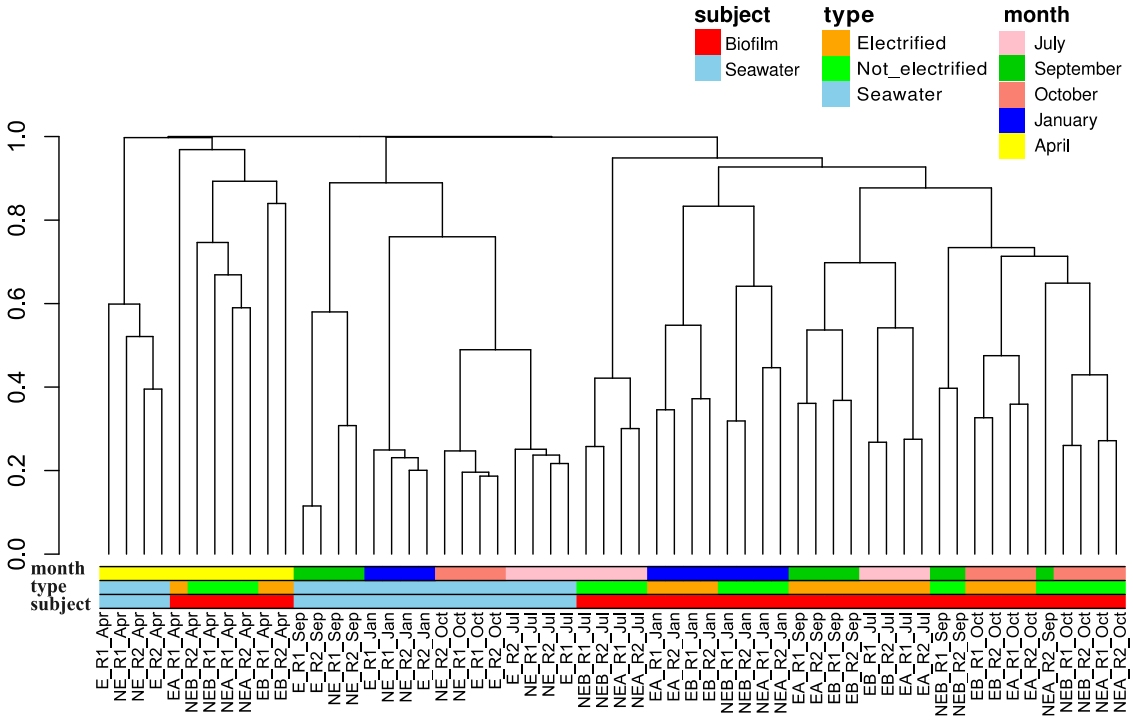

Figure 13. Hierarchical clustering dendrogram of the total ASVs based on Bray-Curtis distance matrix.

To visualize the differences in the prokaryotic assemblages in the samples, a heatmap with cluster analysis was reported in Figure 14.

Flavobacteriaceae and *Rhodobacteraceae* resulted the most abundant families across the entire dataset, with values up to 5.6 and 6.3, respectively. *Desulfobacteraceae* and *Desulfovibrionaceae* were found to be abundant only in biofilm samples collected from not electrified bars in January and April (average abundance of 2.8 and 2.2, respectively).

High dissimilarity between biofilm and seawater samples was observed. Specifically, several taxa including members of the family *Cyanobiaceae*, the

Order SAR 11 Clade I, and the *SAR116 Clade*, were detected almost exclusively in the water samples.

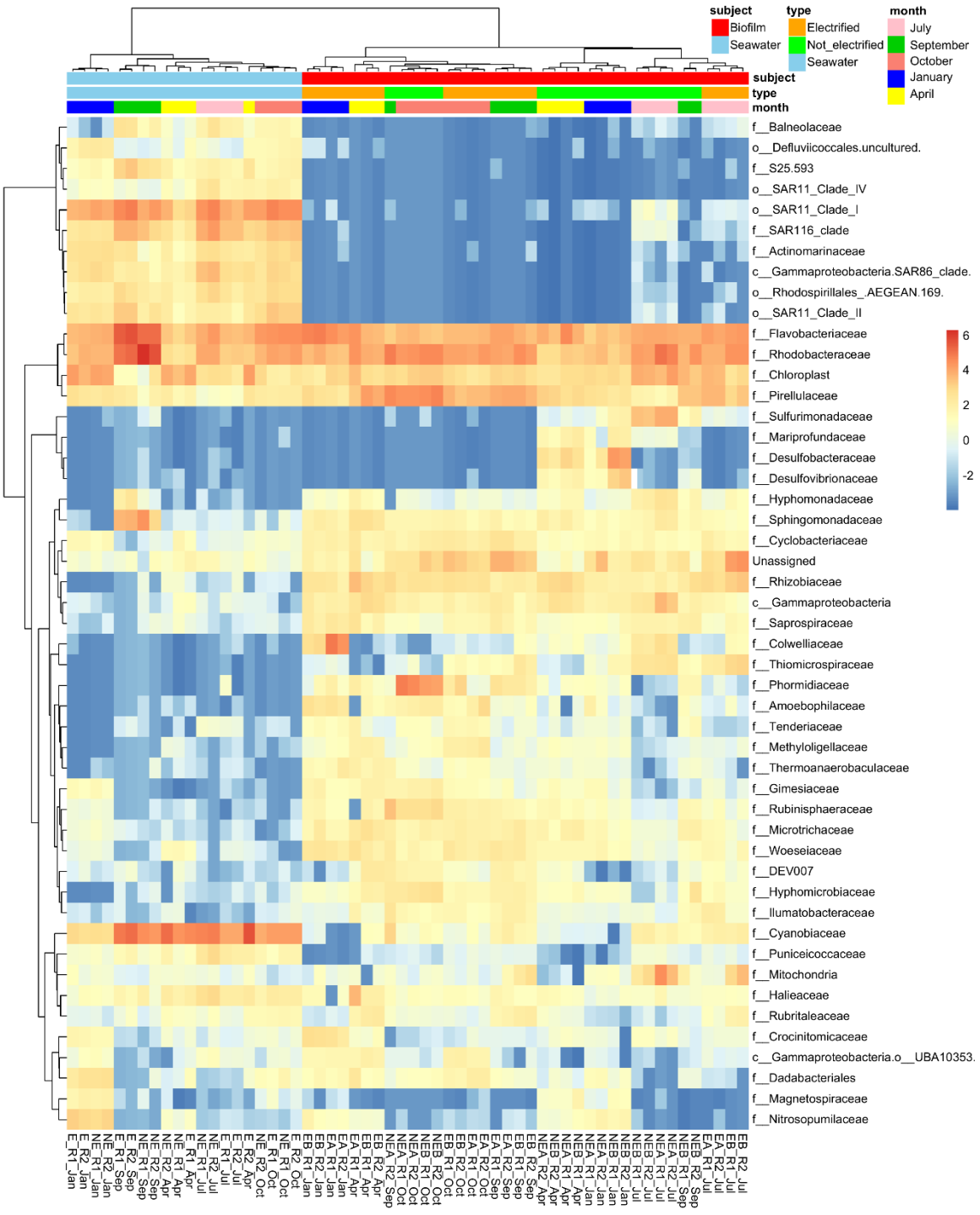

Figure 14. Taxa displaying different abundance values within seawater and biofilm samples collected from electrified and not electrified bars in the different months: July, September,

October, January, April. Relative abundance values are expressed as CLR-transformed values. Metadata associated with each sample are displayed in layers above the heatmap. Samples and taxa were clustered with the ward.D2 method.

The number of shared and exclusive ASVs between biofilm and seawater and within the biofilm samples (between different months, as well as among electrified and not electrified bars) was shown in the Venn diagrams (Figure 15). The total number of ASVs associated with seawater was 4495, while it was 10820 ASVs for the biofilm. Interestingly, only 821 of 14494 ASVs (6%) were common among biofilm and seawater, and 9999 ASVs were exclusively observed in the biofilm samples highlighting the distinct bacterial community found in biofilm (Figure 15a). Among biofilm samples, only 2200 of 10820 ASVs (20%) were shared between electrified and not electrified bars (Figure 15b). Notably, no ASVs were shared among all months (Figure 15c) because April did not have ASVs in common with any of the other months. Each month showed a high number of exclusive ASVs (1100 July, 697 September, 1049 October, 1042 January, and 5234 April). July, September, October, and January shared a total of 296 ASVs. September and October shared 289 ASVs.

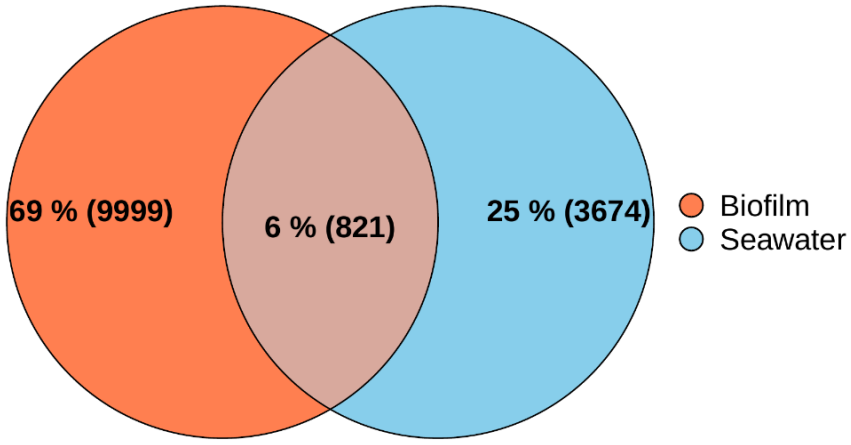

(a)

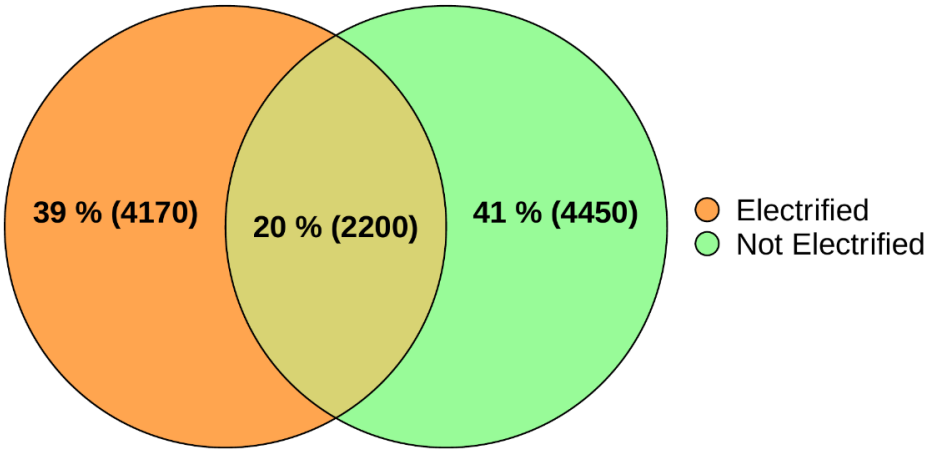

(b)

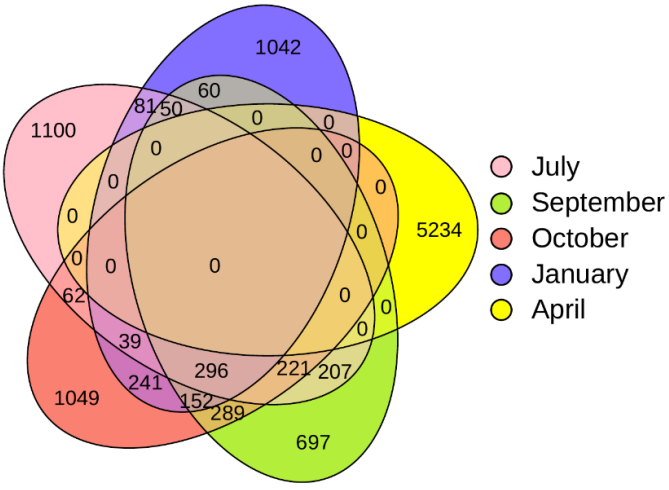

(c)

Figure 15. Venn diagram showing the number of shared and exclusive ASVs between biofilm and seawater (a); among biofilm samples, shared and exclusive ASVs between electrified and not electrified bars (b); among biofilm samples, shared and exclusive ASVs between different months (c).

4.5 Taxonomic composition analysis of biofilm and seawater prokaryotic assemblages

From the analysis of the taxonomic composition of the microbial assemblages present in seawater and in biofilm, microbial groups showed differences in terms of relative contribution to the entire assemblage (Figure 16). *Proteobacteria* was the most abundant phylogenetic group both in seawater and in biofilm samples accounting, on average, for 44% of all sequences. *Proteobacteria* was mainly represented by *Alphaproteobacteria* followed by *Gammaproteobacteria,* which accounted, on average, for 30% and 14% of all sequences, respectively. Among *Alphaproteobacteria, SAR11* and *Rhodobacteraceae* were the two major subgroups. *SAR11* related sequences represented 14% of the whole community obtained from the water samples while it was almost completely absent in the biofilm (on average, 0.09%). *Rhodobacteraceae* was highly present both in seawater and in biofilm samples (on average, 11% and 14% respectively). Among *Proteobacteria* the class *Zetaproteobacteria* was present only in biofilms formed on not electrified bars (on average 0.79%) and totally absent in those on electrified bars. The phylum *Bacteroidetes* was highly abundant, accounting, on average, for 17% of all sequences. Among this phylum, the family *Flavobacteriaceae* was detected in all samples analyzed representing, on average, 13% of all sequences. The

phylum *Cyanobacteria* was more abundant in seawater than in biofilm samples (on average, 20% and 10% of all sequences, respectively). The highest relative abundance of *Cyanobacteria* (43%) in seawater was detected in April compared to the other months (15%, on average). Among this phylum, *Cyanobiaceae* represented 15% of the whole seawater community and was almost absent from the biofilm (0.88%). On the contrary, several taxonomic groups were found to be mainly present in the biofilm samples and less present in seawater. For instance, the phylum *Desulfobacterota* was present mainly in biofilm samples and less in seawater samples (on average 3.11% and 0.16%, respectively). This phylum with its most abundant families (*Desulfobacteraceae*, *Desulfovibrionaceae* and *Desulfobulbaceae*) was mainly present in samples collected from not electrified bars than in those from electrified bars (on average, 5.44% and 0.60%, respectively). Moreover, considering not electrified bars, it was more abundant in January (accounting for 17% of the sequences) than in April (7.64%) and less abundant in the other months (0.71%). The class *Clostridia*, belonging to the phylum *Firmicutes*, was found to be higher abundant (1.20%) in biofilms from not electrified bars compared to the others (0.36%). *Sulfurimonadaceae* and *Arcobacteraceae* belonging to the phylum *Campilobacterota* were mainly present in not

electrified structures (on average, 2.29% and 0.97%, respectively) while absent in electrified structures.

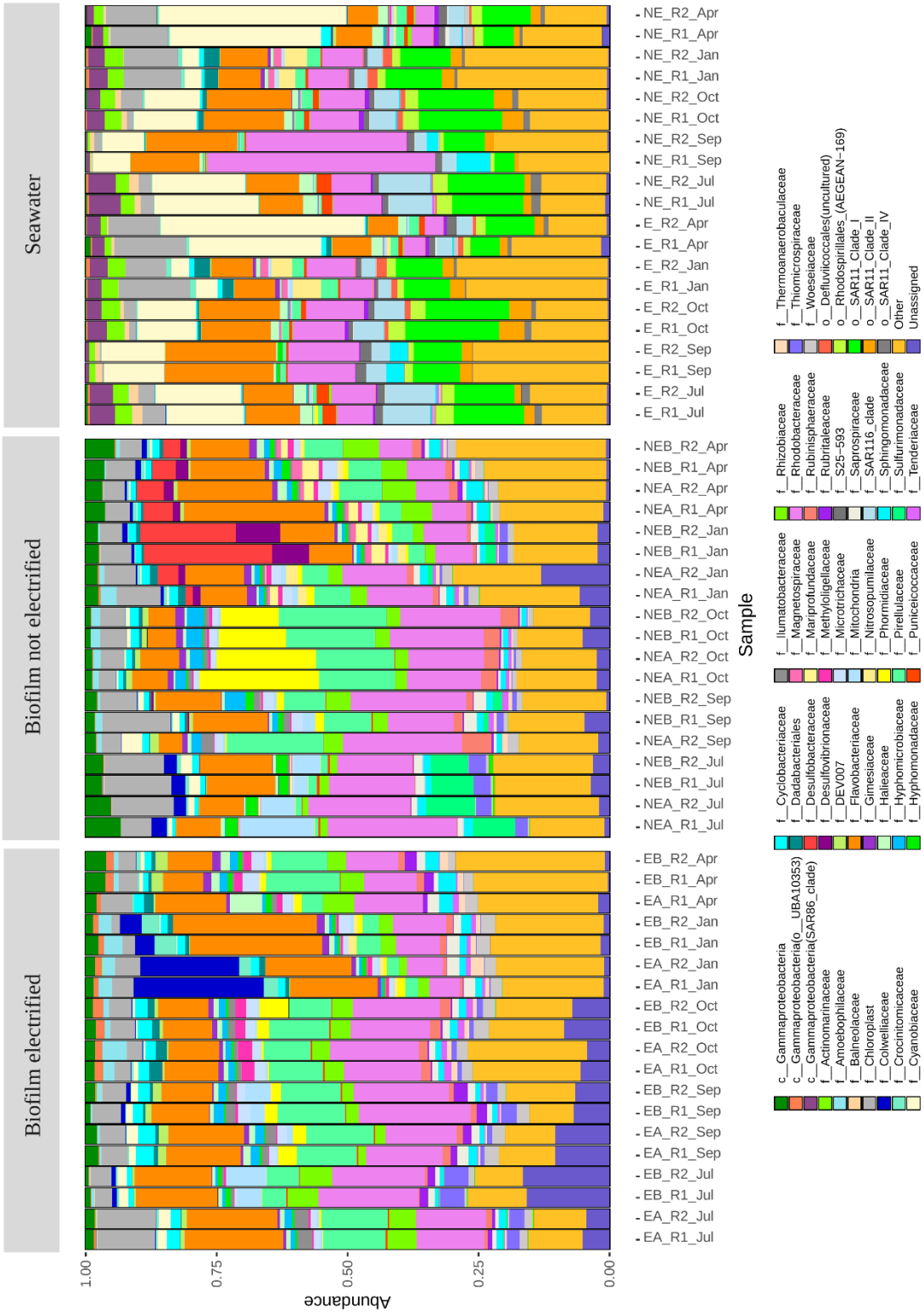

Figure 16. Barplot showing the taxonomic composition of the prokaryotic assemblages present in biofilm and seawater samples at the family level in terms of sequence contribution to each bacterial family. Taxa contributing less than 1% were summed and indicated as "other (< 1%)". Taxa names are preceded by a letter according to the maximum depth of taxonomic assignment: "p" for phylum, "c" for class, "o" for order and "f" for family.

4.6 Alpha and Beta diversity analysis of fungal assemblages

4.6.1 Total ASVs richness

After initial quality filtering and chimera removal, from 1259 to 33551 high-quality sequences were collected from each sample and denoised forming a total of 4528 amplicon sequence variants (ASVs); the total ASVs richness was then calculated from each sample (Figure 17).

Total ASVs richness was similar between biofilm and seawater, ranging from 22 ± 5.6 ASVs to 154.8 ± 24.5 ASVs and from 60.8 ± 29.8 ASVs to 97± 85.9 ASVs, respectively.

Biofilm samples of electrified and not electrified bars showed higher richness in October (106 ± 12.1 ASVs and 154.8 ± 24.5 ASVs, respectively) than in all the other months (ranging from 22 ± 5.6 ASVs to 86.8 ± 9.6 ASVs). The lowest richness was found in January for samples of both electrified and not electrified bars (22 ± 5.6 ASVs and 52.7 ± 10.7 ASVs, respectively).

Seawater samples, as well, showed higher richness in October (97 ± 85.9 ASVs) than in all the other months (ranging from 60.8 ± 29.8 ASVs to 94 ± 25.2 ASVs). The lowest richness was found in January.

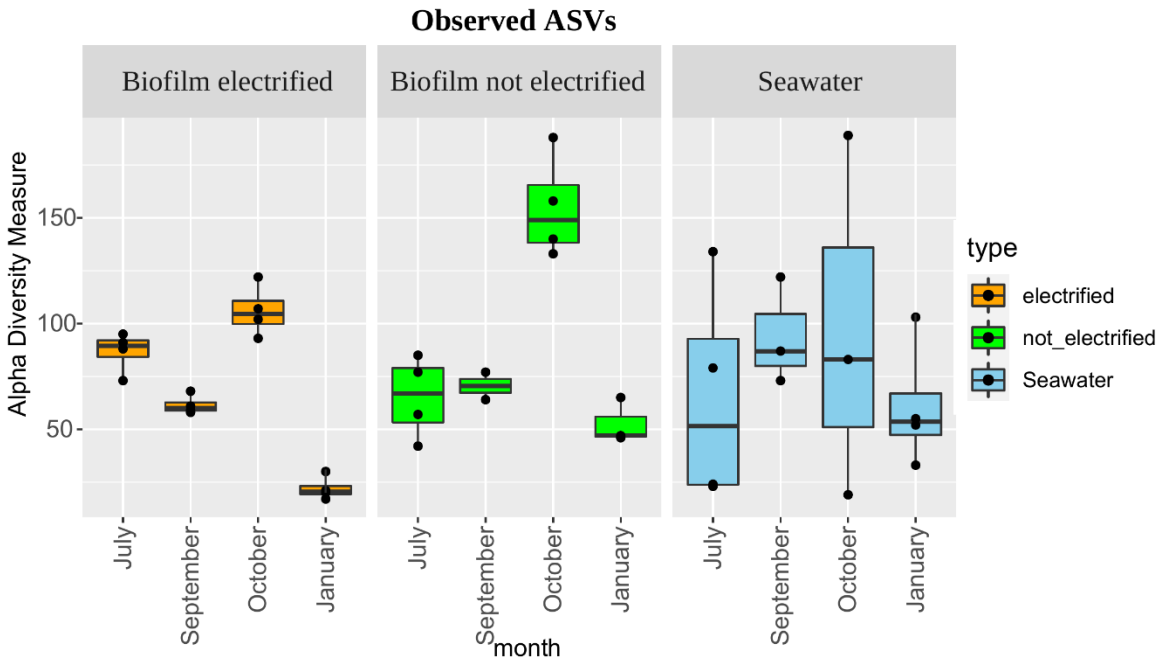

Figure 17. Estimated number of ASVs for each sample.

Differences within the ASVs richness between the different months in both biofilm and seawater samples were supported by rarefaction curve analyses (Figure 18).

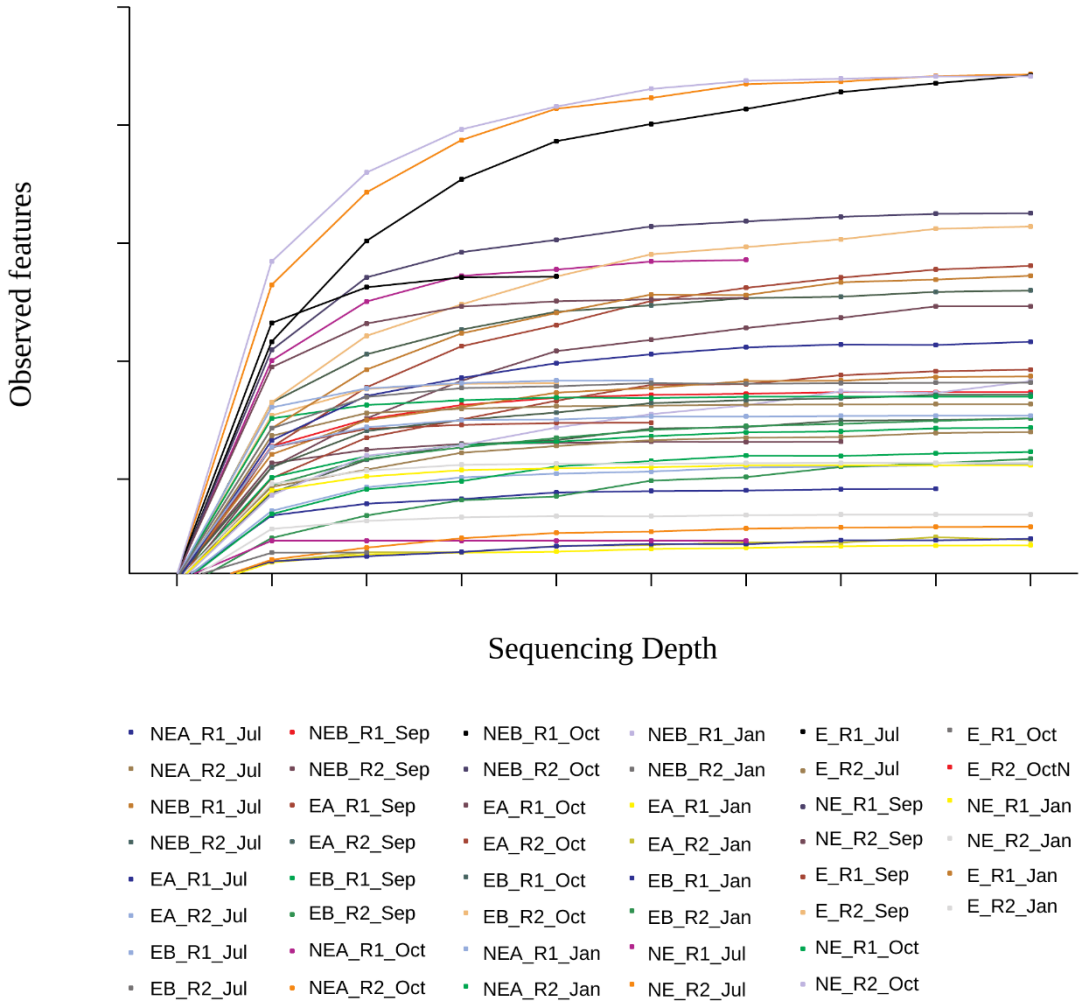

Figure 18. Rarefaction curve of observed ASVs in biofilm and seawater samples.

4.6.2 Alpha diversity indices

The ITS2 metabarcoding analysis in biofilm and seawater samples revealed different Shannon (H'), Pielou's (J), and Simpson (S) indices (Figure 19; Table 5). Shannon weaver index showed a similar pattern between seawater samples and biofilm samples collected from not electrified bars (H' ranging from 2.08 ± 0.28 to 4.04 ± 0.22). For both, higher diversity was found in September and

October (H’ ranging from 3.66 ± 0.91 to 3.68 ± 0.49 and from 3.34 ±0.02 to 4.04 ± 0.22, respectively), compared to the other months.

On the other hand, biofilm samples from electrified bars showed a different pattern with the highest diversity found in July (H’= 3.38 ± 0.46) and the lowest found in January (H’ = 0.97 ± 0.16).

The evenness index showed a similar pattern between seawater samples and biofilm samples from not electrified bars (J ranging from 0.53 ± 0.05 to 0.88 ± 0.03). For both, the highest evenness index was found in October (J = 0.88 ± 0.03 and J = 0.80 ± 0.03, respectively) and the lowest in January (J = 0.63 ± 0.07 and J = 0.53 ± 0.05, respectively). On the contrary, biofilm samples from electrified bars were characterized by a decreasing trend from July, with the highest evenness index (J = 0.76 ± 0.11), to January, with the lowest value (J = 0.31 ± 0.05).

Simpson index showed a similar pattern between seawater samples and biofilm samples from not electrified bars (S ranging from 0.72 ± 0.40 to 0.96 ± 0.01). For both, higher values were found in September and October (S ranging from 0.95 ± 0.03 to 0.95 ± 0.04 and from 0.94 to 0.96 ± 0.01, respectively) compared to the other months. Biofilm samples from electrified bars were characterized by a decreasing trend from July, with the highest Simpson index (S = 0.91 ± 0.08), to January, with the lowest value (S = 0.37 ± 0.06).

	Biofilm Electrified			Biofilm Not Electrified			Seawater		
Month	H’	J	S	H’	J	S	H’	J	S
July	3.38 ±0.46	0.76 ±0.11	0.91 ±0.08	2.94 ±0.38	0.71 ±0.04	0.89 ±0.05	2.65 ±1.63	0.65 ±0.35	0.72 ±0.40
September	2.48 ±0.32	0.60 ±0.09	0.78 ±0.08	3.34 ±0.02	0.79 ±0.03	0.94 ±0.00	3.68 ±0.49	0.81 ±0.07	0.95 ±0.04
October	2.51 ±0.45	0.54 ±0.09	0.73 ±0.10	4.04 ±0.22	0.80 ±0.03	0.96 ±0.01	3.66 ±0.91	0.88 ±0.03	0.95 ±0.03
January	0.97 ±0.16	0.31 ±0.05	0.37 ±0.06	2.08 ±0.28	0.53 ±0.05	0.74 ±0.07	2.54 ±0.51	0.63 ±0.07	0.79 ±0.10

Table 5. Diversity indices used in this study. H', Shannon index; J, Pielou's index; S, Simpson index.

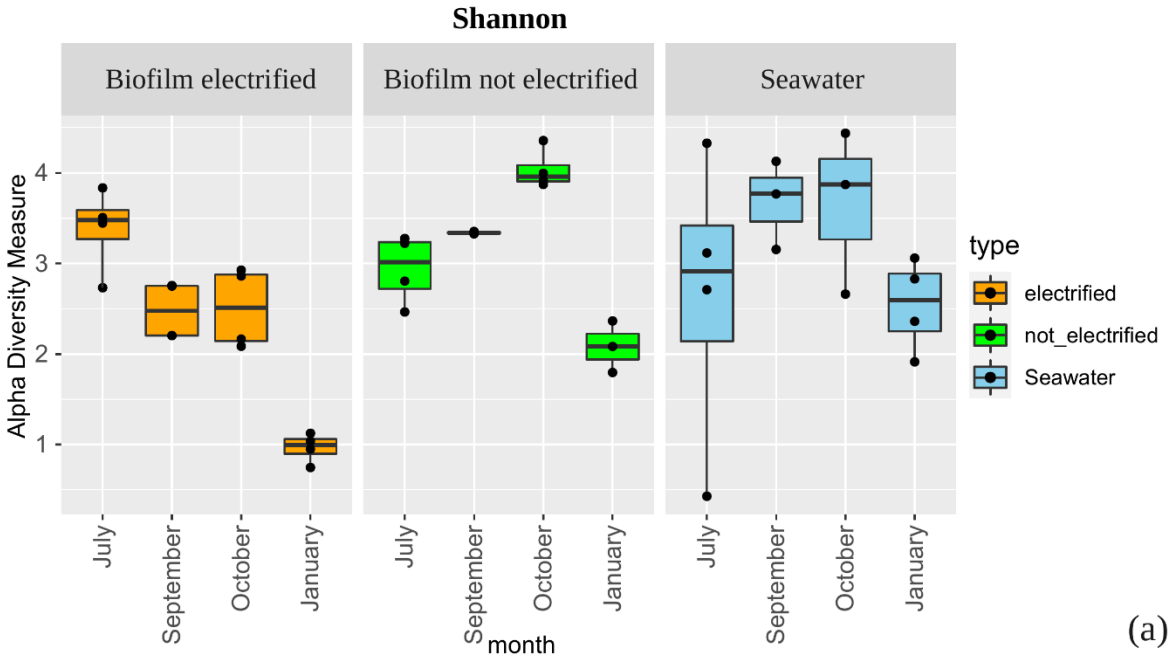

(a)

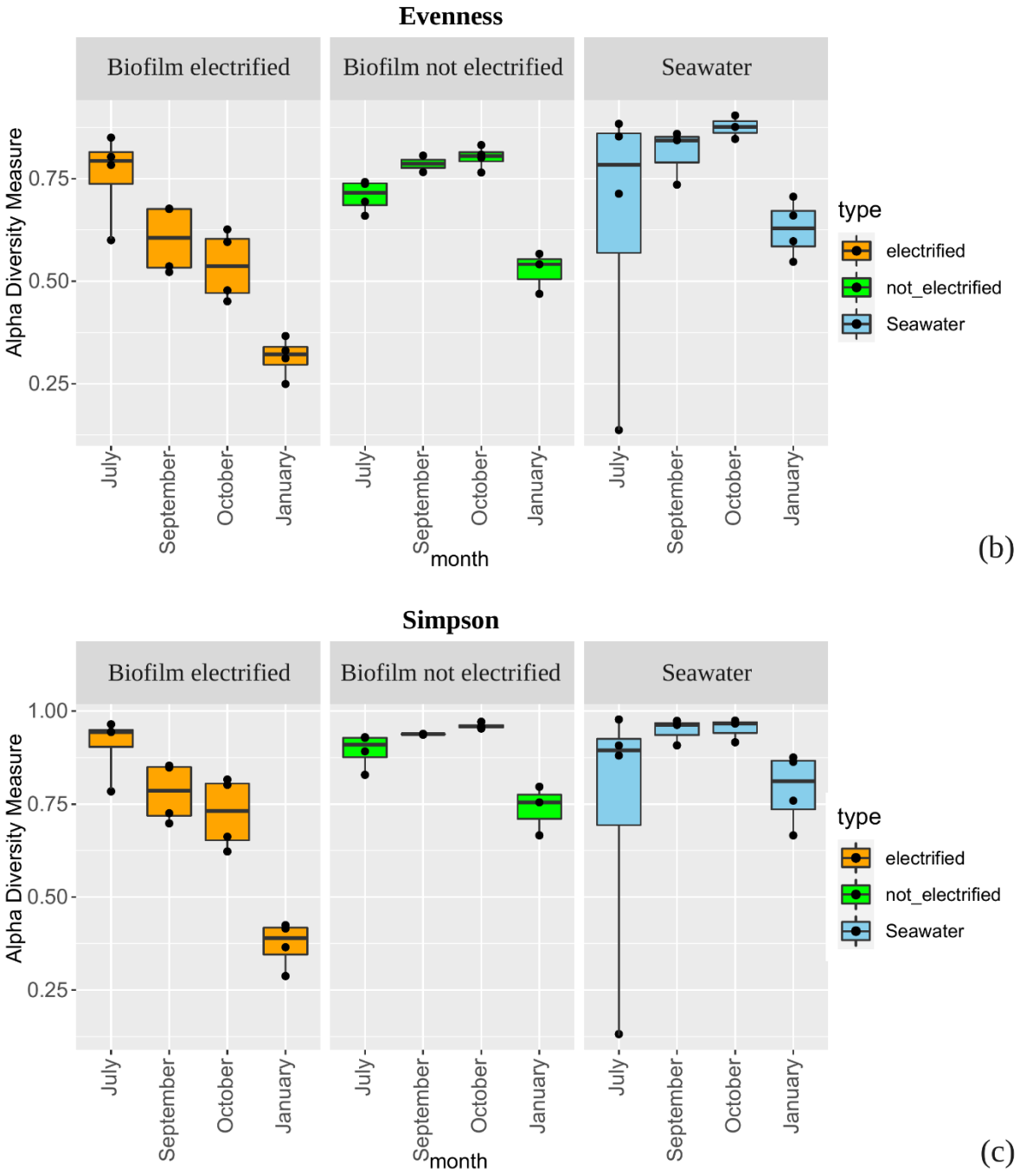

Figure 19. Shannon (a), Pielou's (b), and Simpson (c) indices.

4.6.3 Beta diversity analysis

Principal coordinates analysis (PCoA) ordination based on Bray-Curtis dissimilarity showed the dispersion of fungal community among seawater and biofilm samples and the dispersion within biofilm samples (Figure 20). Seawater and biofilm samples did not display a clear grouping of their fungal assemblages. Instead, a clear clustering pattern resulted for all the samples collected in January (Figure 20a). PCoA of biofilm showed a clustering pattern in July, September, October, and January (Figure 20b). In addition, October and September displayed a grouping pattern based on electrification, whereas samples collected in July and January did not display a clear grouping of their fungal assemblages.

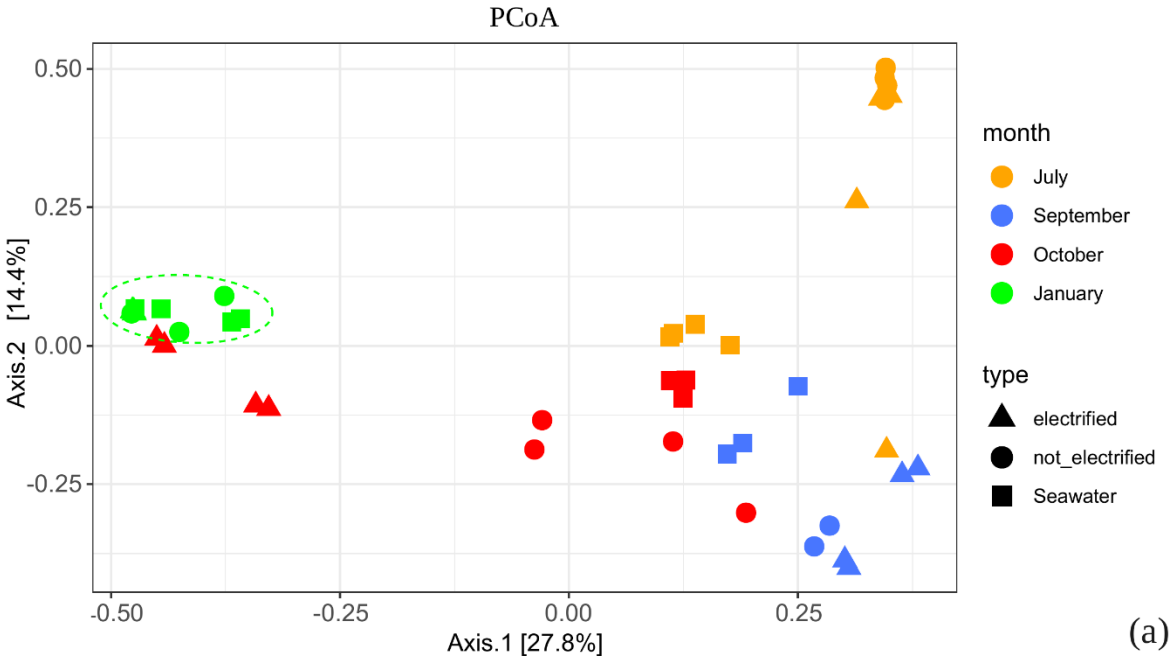

(a)

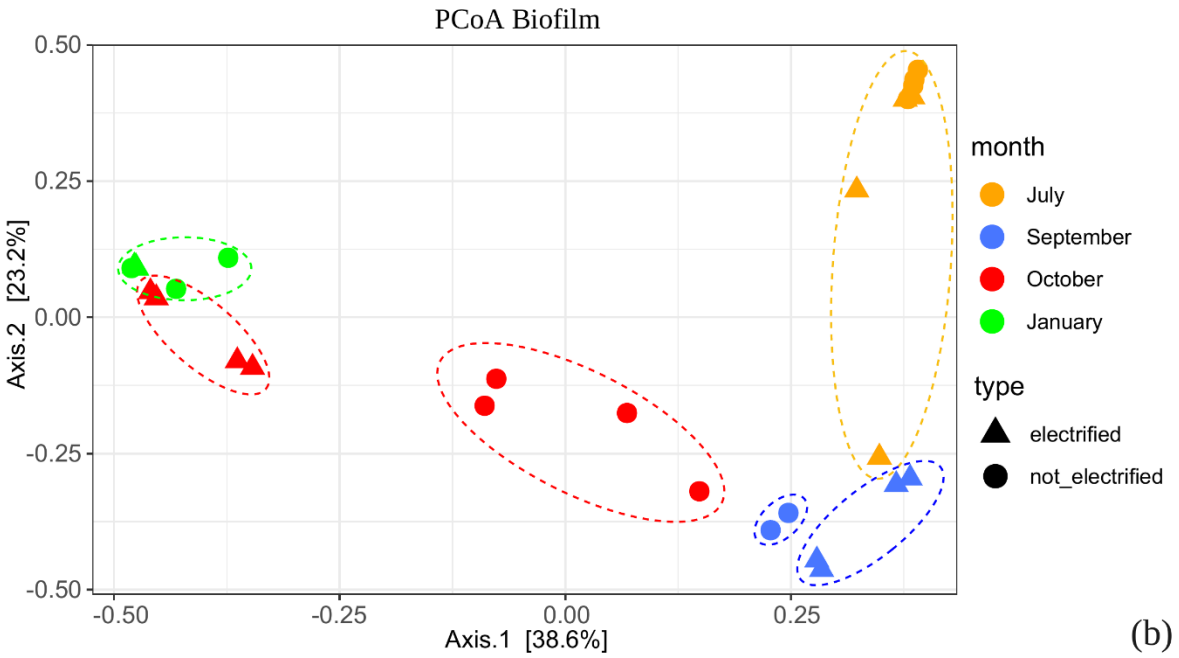

Figure 20. Principal coordinate analysis (PCoA) based on Bray-Curtis dissimilarity matrix of fungal communities associated with seawater and biofilm samples (a) and with biofilm samples (b) collected in different months: July, September, October, January.

The results were further validated by the construction of a hierarchical clustering dendrogram of the total ASVs, based on the Bray-Curtis distance matrix (Figure 21). The dendrogram did not display a clear grouping of fungal assemblages between biofilm and seawater samples. Instead, a clear clustering pattern resulted for all the samples collected in January which showed, on average, 86% dissimilarity with the other months.

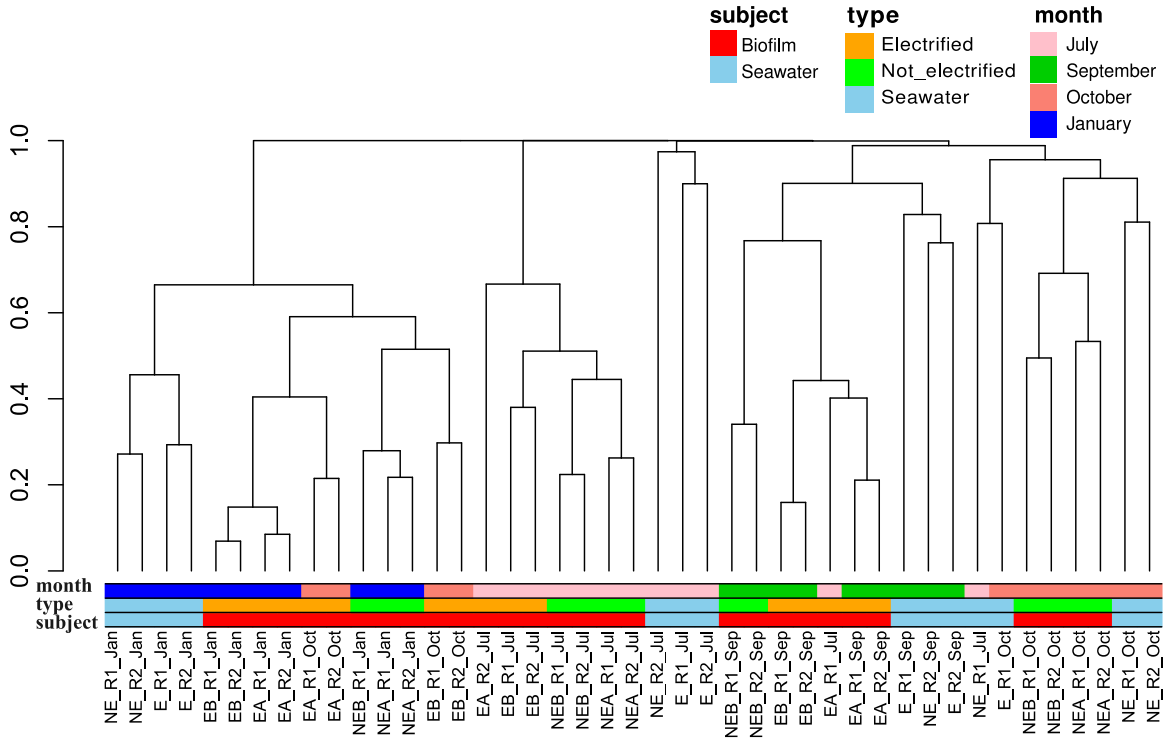

Figure 21. Hierarchical clustering dendrogram of the total ASVs based on Bray-Curtis distance matrix.

Relative abundance values of fungal taxa and their correlations with the type of sample, time, and electrification were reported in the heatmap analysis (Figure 22). The heatmap showed that the phylum *Ascomycota* and, in particular, the order *Pleosporales* were present across the entire dataset, with values up to 6.5 and 5.6, respectively (Figure 22). Among biofilm samples, *Aureobasidium* and *Coprinellus* reached values up to 5.3 and 6.5, respectively. Among seawater and biofilm samples, the phylum *Chytridiomycota* was found to be abundant (abundances up to 6).

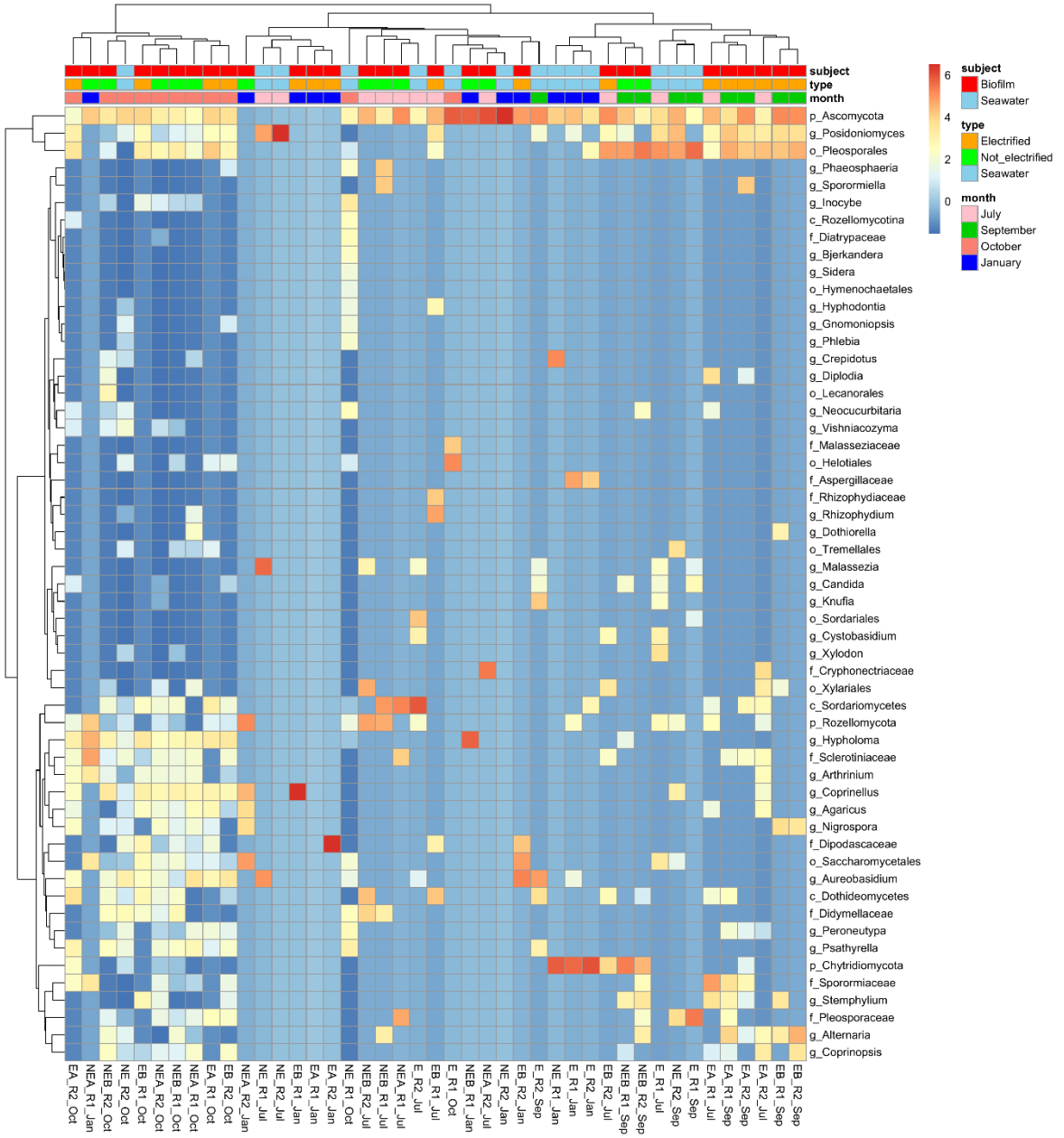

Figure 22. Taxa displaying different abundance values within seawater and biofilm samples collected from electrified and not electrified bars in the different months: July, September, October, January. Relative abundance values, calculated after the removal of unclassified ASVs are expressed as CLR-transformed values. Metadata associated with each sample are displayed in layers above the heatmap. Samples and taxa were clustered with the ward.D2 method.

The number of shared and exclusive ASVs between biofilm and seawater and within the biofilm samples (between different months, as well as among electrified and not electrified bars) was shown in Venn diagrams (Figure 23). The number of ASVs present in all the samples, regardless of their abundance, varied between biofilm and seawater (Figure 23a). Interestingly, only 177 of 1971 ASVs (9%) were common among biofilm and seawater, and 1123 of 1971 ASVs (34%) were exclusively found in the biofilm samples highlighting the distinct fungal community of biofilm. Among biofilm samples, 187 of 1300 ASVs (14%) were shared between electrified and not electrified bars (Figure 23b) and only 4 ASVs were shared among all months (Figure 23c). Each month showed a high number of exclusive ASVs (24% July, 12% September, 45% October, and 8% January). A few ASVs were shared between July, September, and October, whereas no ASVs were in common between July and January.

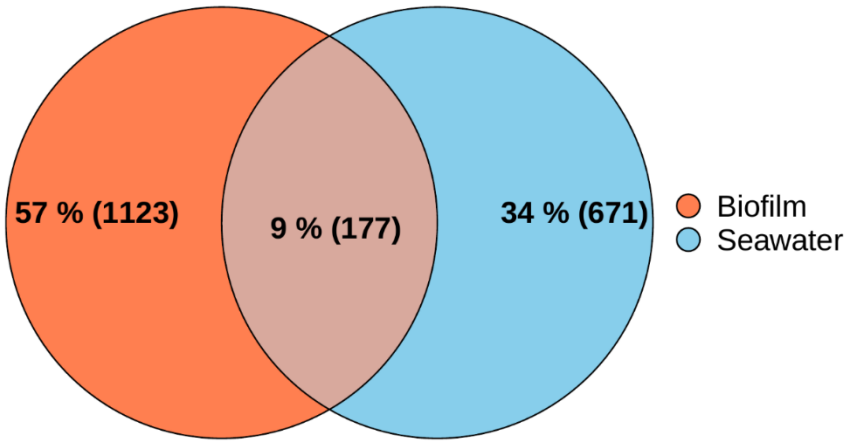

(a)

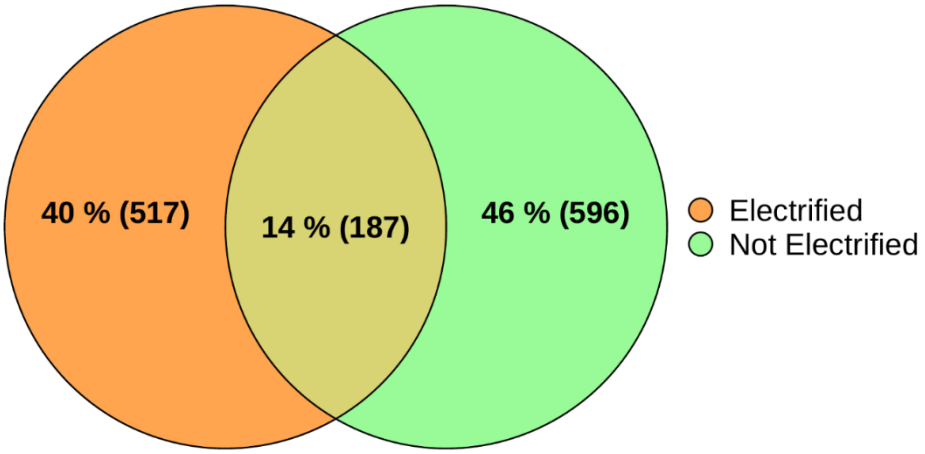

(b)

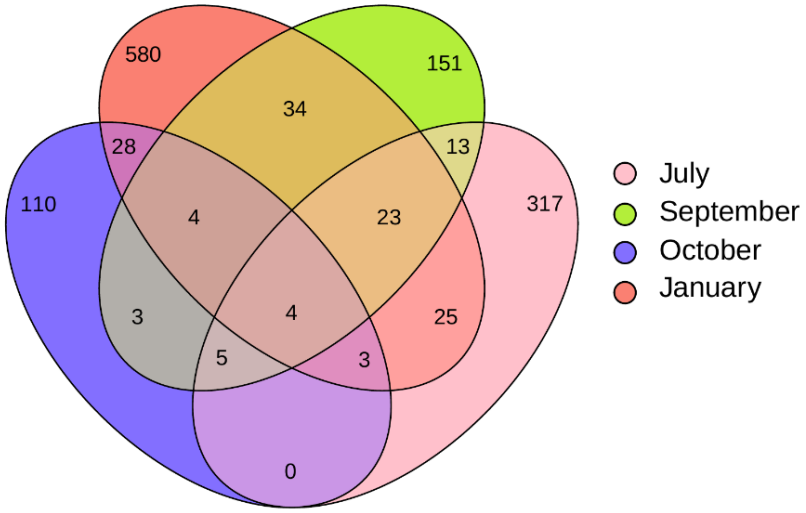

(c)

Figure 23. Venn diagram showing the number of shared and exclusive ASVs between biofilm and seawater (a); among biofilm samples, shared and exclusive ASVs between electrified and not electrified bars (b); among biofilm samples, shared and exclusive ASVs between different months (c).

4.7 Taxonomic composition analysis of biofilm and seawater fungal assemblages

Taxonomic analysis showed that most of the fungal ASVs could not be classified into known fungal taxa (on average ca. 83%, Figure 24). Only a few

ASVs could be affiliated to known fungal taxonomic groups. In particular, the phylum *Ascomycota* was the most represented both in seawater and in biofilm samples, accounting, on average, for 11% of all sequences. Among this phylum, the class *Dothideomycetes*, *Sordariomycetes*, and *Leotiomycetes* were the main abundant (representing, on average, 5.30%, 2.37%, and 0.49% of all sequences, respectively). *Dothideomycetes* were mainly present in September and October (10.8% and 8.1%, respectively) and less in January accounting for 0.15% of all sequences. Among this class, the order *Pleosporales* was the most represented, accounting for 4.10% of all sequences. Within this order, the family *Sporormiaceae* was present only in biofilm samples (on average 0.49%), while it was absent in seawater. Instead, *Pleosporaceae* was detected in seawater with higher values (on average 1.57%) than those found in biofilm samples (on average 0.68%). *Sordariomycetes* reached a very high abundance (51.94%) only in one seawater sample of July compared to all the other samples (on average, 0.63%). Among this class, ASVs belonging to the order *Sordariales* were identified mainly in seawater samples (on average 0.72%) and almost absent in biofilm samples (on average 0.01%). *Leotiomycetes* (mainly represented by the order *Helotiales*) was more abundant in seawater than in biofilm samples (on average 0.74% and 0.36%, respectively).

Basidiomycota accounted, on average, for 3.93% of all sequences and was mainly represented by the class *Agaricomycetes*. This phylum was more abundant in biofilm collected from not electrified bars compared to electrified bars (on average, 4.85% and 2.36%, respectively). Small quantities (0.93% and 0.27%, respectively) of reads were classified as *Chytridiomycota* and *Rozellomycota* phylum which were detected both in seawater and biofilm samples. *Chytridiomycota* was more abundant in biofilm collected from not electrified bars compared to electrified bars (on average, 1.07% and 0.40%, respectively).

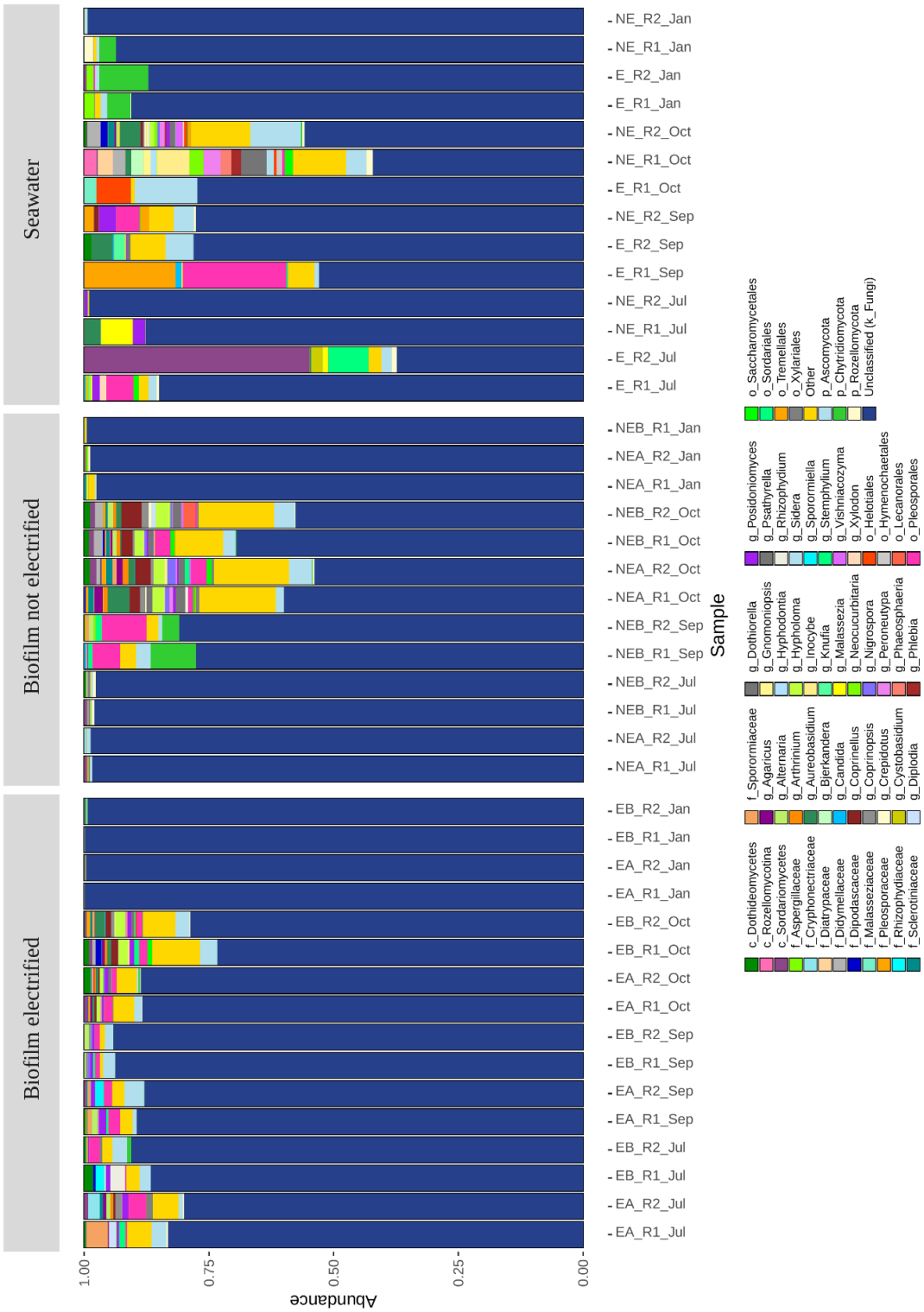

Figure 24. Barplot showing the taxonomic composition of the fungal assemblages present in biofilm and seawater samples at the genus level in terms of sequence contribution to each fungal species. Taxa contributing less than 1% were summed and indicated as "other (< 1%)" Taxa names are preceded by a letter according to the maximum depth of taxonomic assignment: "p" for phylum, "c" for class, "o" for order, "f" for family, and "g" for genus.

5. DISCUSSION

All biotic and abiotic surfaces immersed in seawater are quickly colonized by microorganisms forming complex biofilms (Salamone et al., 2016). Properties of this initial biofilm can influence the trophic relationships, colonization, and recruitment of macrofouling organisms (Antunes et al., 2020). In light of this, understanding the first steps of microfouling colonization is fundamental for a complete view of biological communities that may develop on an artificial reef structure in the marine environment (Salamone et al., 2016). Previous studies have been mainly focused on biofilm formation for improving human health and wellbeing but less for environmental purposes (Bellou et al., 2020).

At the same time, there is evidence that biofilm can damage artificial substrates of industrial plants through corrosive processes resulting in economic impacts (Skovhus et al., 2017). The deterioration of such structures can raise the issue of the potential leaching of contaminants such as PCBs, residual oil, heavy metals, and other toxic substances with impacts on the marine ecosystem and human health (Tornero and Hanke, 2016).

In the present thesis, we provided new insights into the temporal variability of microbial biofilm on two types of substrate: artificial steel structures subject to mineral accretion through electrification technology and non-exposed to electrification. Biofilms and planktonic microbial assemblages in aquatic

environments are very heterogeneous and dynamic, and their composition can be influenced by surrounding environmental parameters such as temperature, salinity, and dissolved oxygen (Elifantz et al., 2013).

Taking into account the fundamental role of microorganisms on biofilm, we investigated the quantitative relevance of microbial biofilm assemblages over five sampling times (from July until April) on electrified and not electrified bars and seawater. As expected, the environmental conditions displayed temporal changes during the sampling period, confirming the seasonal variations in temperature, salinity, and dissolved oxygen, typical of the temperate coastal regions of the Mediterranean Sea (Charles et al., 2005).

Prokaryotic abundances and biomasses within biofilm samples were higher than those of seawater samples as already documented previously (DeLong et al., 1993). Prokaryotic abundances on biofilm samples (from 8.2 x 10^7 to 2 x 10^9 cells g^{-1}) were higher than in previous studies in biofilm developed on PVC panels in the northwestern Mediterranean Sea (7.2 × 10^7 cells.cm^{-2}; Pollet et al., 2018). In seawater samples, prokaryotic abundance (from 5.3 x 10^4 to 2.5 x 10^5 cells ml^{-1}) was similar to that found in the northwestern Mediterranean Sea in past studies (Corinaldesi et al., 2019).

Previous researches investigating the prokaryotic communities in the Central Mediterranean Sea, northwestern Mediterranean Sea, and Adriatic Sea found

that temperature can positively influence prokaryotic abundance (Del Negro et al., 2008; Zaccone et al., 2019; Winter et al., 2009). According to these studies, in our research, the highest prokaryotic abundances and biomasses for both biofilm and seawater samples were found in September when higher temperatures were recorded. In addition, we observed that biofilm collected from not electrified bars reached the lowest prokaryotic abundance and biomass in January, characterized by the lowest temperature. Interestingly, prokaryotic abundances and biomasses of biofilm samples from electrified bars and seawater samples were higher in January than those resulted at the beginning of the experiment (July) and after the turning off of the electrification (April). This could be explained by other factors such as dissolved oxygen, highest in January than in the other months, or the vertical winter mixing responsible for changes in nutrient availability (Zaccone et al., 2019; Winter et al., 2009).

Generally, the composition of the microbial communities attached to solid surfaces is different from that of free-living planktonic assemblages (Bellou et al., 2020). Moreover, the attached bacteria have commonly a higher diversity than in seawater (Antunes et al., 2020). This is consistent with our findings of amplicon sequence variants (ASVs) richness, which displayed higher values for biofilm than for seawater samples.

Our results are consistent with those of previous studies revealing that *Alphaproteobacteria* was the dominant phylogenetic group in both biofilm and seawater samples, comprising 30% of the whole microbial community, followed by the *Gammaproteobacteria* class and the *Bacteroidetes* phylum, which, all together, represented the core biofilm microbiome (Elifantz et al., 2013). Indeed, *Alphaproteobacteria* was the dominant bacterial group in the biofilm, constituting about 26% of the community and mainly composed of *Rhodobacteracea*. This is consistent with previous studies which reported *Alphaproteobacteria* as dominant members in biofilms of coastal waters (Bellou et al., 2020; Salta et al., 2013). Among this phylum, *Rhodobacteracea* members, especially the marine *Roseobacter* genus have been identified as major biofilm components and primary surface colonizers in temperate waters (Bellou et al., 2020). *Bacteroidetes* was also highly abundant and, within this phylum, the dominance of the family *Flavobacteriaceae* was observed, according to past studies (Antunes et al., 2020). The members of this group require high levels of nutrients and organic matter and are reported to be the secondary colonizers (Elifantz et al., 2013).

Oberbeckmann et al. (2016) suggested that the composition of biofilm communities is also driven by seasonal factors. We found an average maximum alpha diversity of all observed indexes during April. Moreover, regarding the

beta diversity, we observed a PCoA analysis clearly separating most spring biofilm samples from all other samples and no ASVs shared between April and the other months in the Venn diagrams. These findings are in line with previous studies which hypothesized a role of spring phytoplankton blooms in the microbial community composition dynamics (Antunes et al., 2020; Elifantz et al., 2013). However, *Rhodobacteraceae* and *Flavobacteriaceae* did not seem to be affected by seasonal variations, since they dominated over the entire investigated period which corroborates their fundamental role as primary and secondary colonizers in marine biofilm formation (Antunes et al., 2020).

Salamone et al. (2016) reported that the composition and the chemical properties of the substrates are other fundamental drivers in marine biofilm development. Considering this, microbial community shifts were expected between not electrified and electrified steel prototypes. In our studies, significant differences were detected comparing both substrates. Herein, we observed the class *Zetaproteobacteria* being present only in biofilms formed on not electrified bars and totally absent in those on electrified bars. This group is composed of iron-oxidizing bacteria known to play a role in the MIC and to provide a suitable microenvironment for anaerobic sulfate-reducing bacteria (SRB) to proliferate (McBeth et al., 2011; Wang et al., 2014). SRB are known to be strongly associated with MIC and include several genera such as:

Desulfovibrio, Desulfomonas, Desulfobulbus, Desulfobacter, Desulfococcus, Desulfosarcina, and *Desulfonema* (Gu, 2019). All these genera belong to the phylum *Desulfobacterota* which was abundant in biofilms collected from not electrified steel, while nearly absent in substrates grown on the electrified bars. Moreover, the class *Clostridia*, known to produce acids resulting in severe damage to the metal, were found to be more abundant (1.2%) in biofilms from not electrified bars compared to the others (0.3%) (Antunes et al., 2020). Interestingly, *Sulfurimonadaceae* and *Arcobacteraceae,* which are sulfur-oxidizing bacteria and thus cause severe corrosion damage to steel surfaces, have been found mainly present in not electrified structures (Skovhus et al., 2017). All these findings were similar to previous studies analysing microbial community successions over steel surfaces (Antunes et al., 2020; McBeth et al., 2011).

Regarding the seawater community, *SAR11* and *Rhodobacteraceae* were the two major subgroups of the *Alphaproteobacteria*. *SAR11* related sequences represented about 14% of the whole community obtained from the water samples while it was almost completely absent in the biofilm since it is considered a planktonic group (Giovannoni and Vergin, 2012). Similar results were obtained for other coastal environments (Elifantz et al., 2013; Rappé et al., 2000). Similarly, *Cyanobiaceae* although representing about 15% of the

whole seawater community, was almost absent from the biofilm. These results suggest that biofilm and planktonic communities are generally distinct despite possessing classes in common. In addition, the percentage of shared ASVs (6%) across the two habitats reflects the high diversification between the prokaryotic communities. The highest relative abundance of *Cyanobacteria* (43%) in seawater was detected in April in contrast with previous studies which reported, for the Mediterranean basin, the lowest relative abundances of this phylum in spring, coincidently with the nano- and micro-phytoplankton spring blooms (Elifantz et al., 2013; Charles et al., 2005; Uysal and Köksalan, 2006). Unfortunately, because of the lack of environmental parameters for April month, we were not able to hypothesize any possible drivers.

The mature biofilm is composed of bacteria, diatoms, benthic dinoflagellates, protozoa, and fungi (Antunes et al., 2020). Fungi are ubiquitous in the marine environment but, despite being considered key players in terrestrial systems, their diversity and ecological function in the aquatic environment remain unexplored (Naim et al., 2017). The fungal abundance in surface seawater sediments is similar to that of soils, thus, considering the importance of soil fungi, it is likely that fungi in marine sediments have an important ecological role (Orsi, 2018). Fungal occurrence is correlated with organic matter, suggesting important roles as recyclers in the ocean (Li et al., 2018). They play

a fundamental part in aquatic food web structures, stability, and functionality through syntrophic to parasitic interactions with other organisms (Grossart et al., 2019). Also, synergistic and antagonistic effects between fungi and bacteria have been demonstrated (Grossart et al., 2019). Despite that, present research generally suffers from a gap in current taxonomic reference databases and in understanding the actual role of these organisms (Naim et al., 2017). Indeed, in our studies, most of the fungal ASVs could not be classified into known fungal taxa (on average ca. 83%) for the lack of curated reference databases (Nilsson et al., 2019). The majority of the fungal taxa inhabiting biofilm belongs to the phylum *Ascomycota* and *Basidiomycota*, which are widespread in different marine environments including also deep-sea extreme ecosystems (Barone et al., 2018; Varrella et al., 2021; Barone et al., 2019; Vargas-Gastélum and Riquelme, 2020). The dominant Ascomycotal classes in both seawater and biofilms were *Dothideomycetes* (with *Pleosporales* being the most common order), *Sordariomycetes*, and *Leotiomycetes*. These fungi have been detected from coastal waters to the deep biosphere, indicating that these classes are ubiquitous in the marine environment (Li et al., 2018). It was reported that Ascomycota may play a great role in the formation of biofilms since, through their metabolism, they consume oxygen efficiently and provide anoxic microhabitats for anaerobic bacteria (Rajala et al., 2016). We found a very low

abundance of this phylum in January, probably related to the winter temperatures highlighting the significant influence of this factor on fungal community development (Li et al., 2018). *Basidiomycota* is generally categorized as filamentous species, able to grow on several substrates (Poli et al., 2018). They are suggested to have a role in the decomposition of recalcitrant molecules such as lignin and tannins allowing large quantities of biomass to return to the marine food web (Poli et al., 2018). Interestingly, we observed that this phylum was less present in the biofilm collected from electrified bars compared to those not electrified. This is coherent with previous studies suggesting that *Basidiomycota* is not common in biofilms developing on limestone substrates (Gómez-Cornelio et al., 2016; Tang and Lian, 2012).

Small quantities (0.9% and 0.3%, respectively) of reads were classified as *Chytridiomycota* and *Rozellomycota* phylum which were detected both in biofilm and seawater samples. The detected quantity of *Chytridiomycota* is consistent with a previous study of the East China Sea (Li et al., 2018).

Some members of this phylum are thought to be pathogens infecting marine algae and animals while *Rozellomycota* can be parasites or hyperparasites of chytrid fungi (Li et al., 2018; Grossart et al., 2019). We observed that *Chytridiomycota* were more abundant in biofilm samples collected from not electrified bars (1.1%) than in those from electrified bars (0.4%). This may

suggest the potential protection of marine algae and animals provided by electrification against pathogenic chytrid fungi.

Overall, we found that the fungal biofilm community was able to efficiently develop on both the substrate types, showing peculiar taxonomic composition and differences with seawater. In addition, we detected heterogeneity in community composition across the different months, therefore, we can hypothesize that this is influenced by different factors including substratum properties, seasonal and temporal changes, and nutrient enrichment (Kirstein et al. 2018; Li et al., 2018). However, most of the fungal assemblage found in biofilm and seawater samples was not taxonomically classified and, for the remaining members, little was found about their role in the marine ecosystem. In light of this, further research is needed to determine fungal diversity, distribution, and ecological role in the marine environment.

6. CONCLUSIONS

Understanding the dynamics of biofilm development is important since it plays a crucial role in driving the subsequent colonization and recruitment of marine invertebrates on different surfaces. In the present thesis, we provide new insights about the effects of mineral accretion technology on the development of bacterial and fungal biofilm communities on marine prototypes with a view to applying this technique in reefing decommissioning offshore oil and gas platforms.

In particular, in the present study, it has been found that:

- prokaryotic abundance of biofilm and seawater microbial assemblages was probably driven by environmental and temporal factors and showed a similar trend between seawater and biofilm samples of both the prototypes.

- the biofilm developed on not electrified prototypes showed a shift in prokaryotic assemblage with the appearance of groups (*Zetaproteobacteria, Desulfobacterota, Clostridia, Sulfurimonadaceae,* and *Arcobacteraceae*) normally responsible for microbiologically influenced corrosion which were almost absent in biofilm on electrified prototypes. This may demonstrate the effectiveness of the mineral accretion technology in providing protection against corrosion.

- differences in microbial assemblages were found between biofilm samples of both the prototypes and seawater samples indicating life-style preferences among members of the microbial communities and the selection of particular members of Bacteria and Fungi for the biofilm formation.
- the fungal biofilm community was able to efficiently develop on both the substrate types, showing peculiar taxonomic composition and differences with seawater. *Chytridiomycota* were less abundant in biofilm collected from electrified prototypes compared to not electrified prototypes suggesting that electrification may provide protection to marine organisms against pathogenic chytrid fungi. However, further research is needed to determine fungal diversity, distribution, and ecological role in the marine environment.

Overall, these results suggest that microbial colonization on electrified prototypes is the first key step and should be taken into account in the next monitoring programs as early indicator for successfully applying the reefing decommissioning offshore oil and gas platforms.

7. REFERENCES

Antunes, J. T., Sousa, A. G., Azevedo, J., Rego, A., Leão, P. N., & Vasconcelos, V. (2020). Distinct temporal succession of bacterial communities in early marine biofilms in a Portuguese Atlantic Port. *Frontiers in microbiology*, *11*, 1938. https://doi.org/10.3389/fmicb.2020.01938

Barone, G., Rastelli, E., Corinaldesi, C., Tangherlini, M., Danovaro, R., & Dell'Anno, A. (2018). Benthic deep-sea fungi in submarine canyons of the Mediterranean Sea. *Progress in Oceanography*, *168*, 57-64. https://doi.org/10.1016/j.pocean.2018.09.011

Barone, G., Varrella, S., Tangherlini, M., Rastelli, E., Dell'Anno, A., Danovaro, R., & Corinaldesi, C. (2019). Marine fungi: Biotechnological perspectives from deep-hypersaline anoxic basins. *Diversity*, *11*(7), 113. https://doi.org/10.3390/d11070113

Bellou, N., Garcia, J. A. L., Colijn, F., & Herndl, G. J. (2020). Seasonality combined with the orientation of surfaces influences the microbial community structure of biofilms in the deep Mediterranean Sea. *Deep Sea Research Part II: Topical Studies in Oceanography*, *171*, 104703. https://doi.org/10.1016/j.dsr2.2019.104703

Bolyen, E., Rideout, J. R., Dillon, M. R., Bokulich, N. A., Abnet, C. C., Al-Ghalith, G. A., ... & Caporaso, J. G. (2019). Reproducible, interactive, scalable and extensible microbiome data science using QIIME 2. *Nature biotechnology*, *37*(8), 852-857. https://doi.org/10.1038/s41587-019-0209-9

Britton, J., & Taylor, M. L. (2017). Advancements in Cathodic Protection of offshore structures. *Trends in Oil and Gas Corrosion Research and Technologies: Production and Transmission*, 593–612. https://doi.org/10.1016/B978-0-08-101105-8.00025-5

Bull, A. S., & Love, M. S. (2019). Worldwide oil and gas platform decommissioning: A review of practices and reefing options. *Ocean & Coastal Management*, *168*, 274–306. https://doi.org/10.1016/J.OCECOAMAN.2018.10.024

Callahan, B. J., McMurdie, P. J., Rosen, M. J., Han, A. W., Johnson, A. J. A., & Holmes, S. P. (2016). DADA2: high-resolution sample inference from

Illumina amplicon data. *Nature methods*, *13*(7), 581-583. https://doi.org/10.1038/nmeth.3869

Capobianco, N., Basile, V., Loia, F., & Vona, R. (2021). Toward a sustainable decommissioning of offshore platforms in the oil and gas industry: A pestle analysis. Sustainability (Switzerland), 13(11). https://doi.org/10.3390/su13116266

Charles, F., Lantoine, F., Brugel, S., Chrétiennot-Dinet, M. J., Quiroga, I., & Rivière, B. (2005). Seasonal survey of the phytoplankton biomass, composition and production in a littoral NW Mediterranean site, with special emphasis on the picoplanktonic contribution. *Estuarine, Coastal and Shelf Science*, *65*(1-2), 199-212. https://doi.org/10.1016/j.ecss.2005.06.006

Claisse, J. T., Pondella, D. J., Love, M., Zahn, L. A., Williams, C. M., Williams, J. P., & Bull, A. S. (2014). Oil platforms off California are among the most productive marine fish habitats globally. *Proceedings of the National Academy of Sciences of the United States of America*, *111*(43), 15462–15467. https://doi.org/10.1073/pnas.1411477111

Corinaldesi, C., Rastelli, E., Canensi, S., Tangherlini, M., Danovaro, R., & Dell'Anno, A. (2019). High rates of viral lysis stimulate prokaryotic turnover and C recycling in bathypelagic waters of a Ligurian canyon (Mediterranean Sea). *Progress in Oceanography*, *171*, 70-75. https://doi.org/10.1016/j.pocean.2018.12.017

Danovaro, R. (2010). *Methods for the Study of Deep-sea Sediments, their Functioning and Biodiversity*. CRC press. https://doi.org/10.1201/9781439811382

Danovaro, R., Dell'Anno, A., Corinaldesi, C., Rastelli, E., Cavicchioli, R., Krupovic, M., Noble R. T., Nunoura T., & Prangishvili, D. (2016). Virus-mediated archaeal hecatomb in the deep seafloor. *Science Advances*, *2*(10), e1600492. https://doi.org/10.1126/sciadv.1600492

de Gómez Saravia, S. G., de Mele, M. F. L., Videla, H. A., & Edyvean, R. G. J. (1997). Bacterial biofilms on cathodically protected stainless steel. *Biofouling*, *11*(1), 1–17. https://doi.org/10.1080/08927019709378317

Del Negro, P., Celussi, M., Crevatin, E., Paoli, A., Bernardi Aubry, F., & Pugnetti, A. (2008). Spatial and temporal prokaryotic variability in the northern

Adriatic Sea. *Marine Ecology*, *29*(3), 375-386. https://doi.org/10.1111/j.1439-0485.2008.00249.x

DeLong, E. F., Franks, D. G., & Alldredge, A. L. (1993). Phylogenetic diversity of aggregate-attached vs. free-living marine bacterial assemblages. *Limnology and oceanography*, *38*(5), 924-934. https://doi.org/10.4319/lo.1993.38.5.0924
Edgar, R. C. (2018). Accuracy of taxonomy prediction for 16S rRNA and fungal ITS sequences. *PeerJ*, *6*, e4652. https://doi.org/10.7717/peerj.4652

Edyvean, R. G. J. (1984). Interactions between microfouling and the calcareous deposit formed on cathodically protected steel in sea water. *Marine Corrosion and Fouling,*, *2*, 469-483.

Edyvean, R. G. J., Maines, A. D., Hutchinson, C. J., Silk, N. J., & Evans, L. v. (1992). Interactions between cathodic protection and bacterial settlement on steel in seawater. *International Biodeterioration & Biodegradation*, *29*(3–4), 251–271. https://doi.org/10.1016/0964-8305(92)90047-R

Elenco Delle Piattaforme Marine e Strutture Assimilabili-Ministero dello sviluppo economico DGS UNMIG. Retrieved 29 November 2021, from https://unmig.mise.gov.it/images/dati/piattaforme.pdf.

Elifantz, H., Horn, G., Ayon, M., Cohen, Y., & Minz, D. (2013). Rhodobacteraceae are the key members of the microbial community of the initial biofilm formed in Eastern Mediterranean coastal seawater. *FEMS microbiology ecology*, *85*(2), 348-357. https://doi.org/10.1111/1574-6941.12122

El-Reedy, M. A. (2020). Corrosion protection. *Offshore Structures*, 359–417. https://doi.org/10.1016/B978-0-12-816191-3.00006-7

Fabi, G., Grati, F., Puletti, M., & Scarcella, G. (2004). Effects on fish community induced by installation of two gas platforms in the Adriatic Sea. *Marine Ecology Progress Series*, *273*, 187-197. https://doi.org/10.3354/meps273187

Ferreira, D. F., & Suslick, S. B. (2001). Identifying potential impacts of bonding instruments on offshore oil projects. *Resources Policy*, *27*(1), 43–52. https://doi.org/10.1016/S0301-4207(01)00007-1

Fowler, A. M., & Booth, D. J. (2012). Evidence of sustained populations of a small reef fish on artificial structures. Does depth affect production on artificial

reefs? *Journal of Fish Biology*, *80*(3), 613–629. https://doi.org/10.1111/j.1095-8649.2011.03201.x

Fowler, A. M., Jørgensen, A. M., Svendsen, J. C., Macreadie, P. I., Jones, D. O., Boon, A. R., ... & Coolen, J. W. (2018). Environmental benefits of leaving offshore infrastructure in the ocean. Frontiers in Ecology and the Environment, 16(10), 571-578. https://doi.org/10.1002/fee.1827

Gazzetta Ufficiale Della Repubblica Italiana. Retrieved 29 November 2021, from https://www.gazzettaufficiale.it/eli/id/2019/03/08/19A01522/sg

Gihring, T. M., Green, S. J., & Schadt, C. W. (2012). Massively parallel rRNA gene sequencing exacerbates the potential for biased community diversity comparisons due to variable library sizes. *Environmental microbiology*, *14*(2), 285-290. https://doi.org/10.1111/j.1462-2920.2011.02550.x

Giovannoni, S. J., & Vergin, K. L. (2012). Seasonality in ocean microbial communities. *Science*, *335*(6069), 671-676. https://doi.org/10.1126/science.1198078

Gómez-Cornelio, S., Ortega-Morales, O., Morón-Ríos, A., Reyes-Estebanez, M., & Rosa-García, S. D. L. (2016). Changes in fungal community composition of biofilms on limestone across a chronosequence in Campeche, Mexico. *Acta botánica mexicana*, (117), 59-77. https://doi.org/10.21829/abm117.2016.1168

Goreau, T. J. (2014). Electrical Stimulation Greatly Increases Settlement, Growth, Survival, and Stress Resistance of Marine Organisms. *Natural Resources*, *05*(10), 527–537. https://doi.org/10.4236/nr.2014.510048

Goreau, T. J., & Trench, R. Kent. (2013). Innovative methods of marine ecosystem restoration. CRC Press. https://doi.org/10.1201/b14314

Grossart, H. P., Van den Wyngaert, S., Kagami, M., Wurzbacher, C., Cunliffe, M., & Rojas-Jimenez, K. (2019). Fungi in aquatic ecosystems. *Nature Reviews Microbiology*, *17*(6), 339-354. https://doi.org/10.1038/s41579-019-0175-8

Gu, J. D. (2019). Corrosion, Microbial. *Encyclopedia of Microbiology*, 762–771. https://doi.org/10.1016/B978-0-12-809633-8.13026-2

Gu, J. D., Ford, T. E., Mitton, D. B., & Mitchell, R. (2000). Microbial corrosion of metals. *The Uhlig Corrosion Handbook. 2nd Edition. New York: Wiley*, 915-27.

Hamzah, B. A. (2003). International rules on decommissioning of offshore installations: some observations. Marine Policy, 27(4), 339–348. https://doi.org/10.1016/S0308-597X(03)00040-X

Henrion, M., Bernstein, B., & Swamy, S. (2015). A multi-attribute decision analysis for decommissioning offshore oil and gas platforms. *Integrated Environmental Assessment and Management*, *11*(4), 594–609. https://doi.org/10.1002/ieam.1693

Hernandez, G., Hartt, H., & Videla, H. A. (1992). Biofilms and their influence on cathodic protection: A literature survey. In *Proc., 1st Pan American Corrosion and Protection Congress, Mar del Plata, Argentina* (Vol. 2, p. 391). https://doi.org/10.1515/CORRREV.1994.12.1-2.29

Hilbertz, W. H. (1979). Electrodeposition of Minerals in Sea Water: Experiments and Applications. In *IEEE JOURNAL ON OCEANIC ENGINEERING* (Issue 3). https://doi.org/10.1109/JOE.1979.1145428

Hilbertz, W. H. (1981). Mineral accretion of large surface structures, building components and elements. *U.S. Patent No. 4,246,075*.

Hilbertz, Wolf H., and Thomas J. Goreau. (1996). Method of enhancing the growth of aquatic organisms, and structures created thereby. *U.S. Patent No. 5,543,034*.

Hughes, J. B., & Hellmann, J. J. (2005). The application of rarefaction techniques to molecular inventories of microbial diversity. *Methods in enzymology*, *397*, 292-308. https://doi.org/10.1016/S0076-6879(05)97017-1

Hunsucker, K., Melnikov, A., Gilligan, M., Gardner, H., Erdogan, C., Weaver, R., & Swain, G. (2021). Cathodically protected steel as an alternative to plastic for oyster restoration mats. *Ecological Engineering*, *164*, 106210. https://doi.org/10.1016/J.ECOLENG.2021.106210

International Maritime Organization. Imo.org. (2021). Retrieved 29 November 2021, from https://www.imo.org/

Istanbullu, O., Babauta, J., Duc Nguyen, H., & Beyenal, H. (2012). Electrochemical biofilm control: mechanism of action. *Biofouling*, *28*(8), 769-778. https://doi.org/10.1080/08927014.2012.707651

Karoui, H., Riffault, B., Jeannin, M., Kahoul, A., Gil, O., ben Amor, M., & Tlili, M. M. (2013). Electrochemical scaling of stainless steel in artificial

seawater: Role of experimental conditions on CaCO3 and Mg(OH)2 formation. *Desalination*, *311*, 234–240. https://doi.org/10.1016/J.DESAL.2012.07.011

Kirstein, I. V., Wichels, A., Krohne, G., & Gerdts, G. (2018). Mature biofilm communities on synthetic polymers in seawater-Specific or general?. *Marine Environmental Research*, *142*, 147-154. https://doi.org/10.1080/08927014.2012.707651

Kolde, R. (2019). pheatmap: Pretty Heatmaps. R package version 1.0.12. https://CRAN.R-project.org/package=pheatmap

Lahti, L., Shetty, S. (2017). microbiome R package. https://doi.org/10.18129/B9.bioc.microbiome

Lakhal, S. Y., Khan, M. I., & Islam, M. R. (2009). An "Olympic" framework for a green decommissioning of an offshore oil platform. *Ocean and Coastal Management*, *52*(2), 113–123. https://doi.org/10.1016/j.ocecoaman.2008.10.007

Langhamer, O. (2012). Artificial reef effect in relation to offshore renewable energy conversion: State of the art. In The Scientific World Journal (Vol. 2012). https://doi.org/10.1100/2012/386713

Larsson, J. (2018). eulerr: Area-Proportional Euler Diagrams with Ellipses. https://CRAN.R-project.org/package=eulerr

Legal.un.org. (2021). Retrieved 29 November 2021, from https://legal.un.org/ilc/texts/instruments/english/conventions/8_1_1958_continental_shelf.pdf.

Li, K., Whitfield, M., & Van Vliet, K. J. (2013). Beating the bugs: roles of microbial biofilms in corrosion. *Corrosion Reviews*, *31*(3-6), 73-84. https://doi.org/10.1515/corrrev-2013-0019

Li, W., Wang, M., Pan, H., Burgaud, G., Liang, S., Guo, J., ... & Cai, L. (2018). Highlighting patterns of fungal diversity and composition shaped by ocean currents using the East China Sea as a model. *Molecular ecology*, *27*(2), 564-576. https://doi.org/10.1111/mec.14440

Liduino, V., Galvão, M., Brasil, S., & Sérvulo, E. (2021). SRB-mediated corrosion of marine submerged AISI 1020 steel under impressed current

cathodic protection. *Colloids and Surfaces B: Biointerfaces*, *202*, 111701. https://doi.org/10.1016/J.COLSURFB.2021.111701

Lin, J., & Ballim, R. (2012). Biocorrosion control: Current strategies and promising alternatives. *African Journal of Biotechnology*, *11*(91), 15736-15747. https://doi.org/10.5897/AJB12.2479

Little, B. J., & Ray, R. I. (2002). The role of fungi in microbiologically influenced corrosion. *Naval Research lab Stennis Space Center MS.*

Little, B. J., & Wagner, P. A. (1995). Interrelationship between marine biofouling, cathodic protection and microbiologically influenced corrosion. *Materials Science Forum*, *192–194*(pt 1), 433–446. https://doi.org/10.4028/www.scientific.net/msf.192-194.433

Love, M. S., Schroeder, D. M., Lenarz, W., MacCall, A., Bull, A. S., & Thorsteinson, L. (2006). Potential use of offshore marine structures in rebuilding an overfished rockfish species, bocaccio (Sebastes paucispinis). *Fishery Bulletin*, *104*(3), 383-390.

Lv, M., Du, M., & Li, Z. (2022). Investigation of mixed species biofilm on corrosion of X65 steel in seawater environment. *Bioelectrochemistry*, *143*, 107951. https://doi.org/10.1016/J.BIOELECHEM.2021.107951

Macreadie, P. I., Fowler, A. M., & Booth, D. J. (2011). Rigs-to-reefs: Will the deep sea benefit from artificial habitat? In *Frontiers in Ecology and the Environment* (Vol. 9, Issue 8, pp. 455–461). https://doi.org/10.1890/100112

Margheritini, L., Colaleo, G., Contestabile, P., Bjørgård, T. L., Simonsen, M. E., Lanfredi, C., Dell'Anno, A., & Vicinanza, D. (2020). Development of an eco-sustainable solution for the second life of decommissioned oil and gas platforms: The mineral accretion technology. *Sustainability (Switzerland)*, *12*(9). https://doi.org/10.3390/su12093742

Martin, M. (2011). Cutadapt removes adapter sequences from high-throughput sequencing reads. *EMBnet. journal*, *17*(1), 10-12. https://doi.org/10.14806/ej.17.1.200

McBeth, J. M., Little, B. J., Ray, R. I., Farrar, K. M., & Emerson, D. (2011). Neutrophilic iron-oxidizing "Zetaproteobacteria" and mild steel corrosion in nearshore marine environments. *Applied and Environmental*

Microbiology, *77*(4), 1405-1412. https://doi.org/10.1128/AEM.02095-10

McMurdie, P. J., & Holmes, S. (2013). phyloseq: an R package for reproducible interactive analysis and graphics of microbiome census data. *PloS one*, *8*(4), e61217. https://doi.org/10.1371/journal.pone.0061217.g001

Medihala, P. G., Lawrence, J. R., Swerhone, G. D. W., & Korber, D. R. (2013). Transient response of microbial communities in a water well field to application of an impressed current. *Water Research*, *47*(2), 672–682. https://doi.org/10.1016/J.WATRES.2012.10.049

Naim, M. A., Smidt, H., & Sipkema, D. (2017). Fungi found in Mediterranean and North Sea sponges: how specific are they?. *PeerJ*, *5*, e3722. https://doi.org/10.7717/peerj.3722

Nilsson, R. H., Anslan, S., Bahram, M., Wurzbacher, C., Baldrian, P., & Tedersoo, L. (2019). Mycobiome diversity: high-throughput sequencing and identification of fungi. *Nature Reviews Microbiology*, *17*(2), 95-109. https://doi.org/10.1038/s41579-018-0116-y

Nilsson, R. H., Larsson, K. H., Taylor, A. F. S., Bengtsson-Palme, J., Jeppesen, T. S., Schigel, D., ... & Abarenkov, K. (2019). The UNITE database for molecular identification of fungi: handling dark taxa and parallel taxonomic classifications. *Nucleic acids research*, *47*(D1), D259-D264. https://doi.org/10.1093/nar/gky1022

Oberbeckmann, S., Osborn, A. M., & Duhaime, M. B. (2016). Microbes on a bottle: substrate, season and geography influence community composition of microbes colonizing marine plastic debris. *PLoS One*, *11*(8), e0159289. https://doi.org/10.1371/journal.pone.0159289

Oksanen, J., F., Blanchet, G., Friendly, M., Kindt, R., Legendre, P., McGlinn, D., Minchin. P. R., O'Hara, B., Simpson, G. L., Solymos, P., Stevens, M. H. H., Szoecs, E., and Wagner, H., (2020). The vegan package: *Community ecology package*

Orsi, W. D. (2018). Ecology and evolution of seafloor and subseafloor microbial communities. *Nature Reviews Microbiology*, *16*(11), 671-683. https://doi.org/10.1038/s41579-018-0046-8

Parada, A. E., Needham, D. M., & Fuhrman, J. A. (2016). Every base matters: assessing small subunit rRNA primers for marine microbiomes with mock communities, time series and global field samples. *Environmental microbiology*, *18*(5), 1403-1414. https://doi.org/10.1111/1462-2920.13023

Parente, V., Ferreira, D., Moutinho dos Santos, E., & Luczynski, E. (2006). Offshore decommissioning issues: Deductibility and transferability. Energy Policy, 34(15), 1992–2001. https://doi.org/10.1016/j.enpol.2005.02.008

Poli, A., Vizzini, A., Prigione, V., & Varese, G. C. (2018). Basidiomycota isolated from the Mediterranean Sea–Phylogeny and putative ecological roles. *Fungal Ecology*, *36*, 51-62. https://doi.org/10.1016/j.funeco.2018.09.002

Pollet, T., Berdjeb, L., Garnier, C., Durrieu, G., Le Poupon, C., Misson, B., & Briand, J. F. (2018). Prokaryotic community successions and interactions in marine biofilms: the key role of Flavobacteriia. *FEMS microbiology ecology*, *94*(6), fiy083. https://doi.org/10.1093/femsec/fiy083

Price, M. N., Dehal, P. S., & Arkin, A. P. (2010). FastTree 2–approximately maximum-likelihood trees for large alignments. *PloS one*, *5*(3), e9490. https://doi.org/10.1371/journal.pone.0009490

Quast, C., Pruesse, E., Yilmaz, P., Gerken, J., Schweer, T., Yarza, P., ... & Glöckner, F. O. (2012). The SILVA ribosomal RNA gene database project: improved data processing and web-based tools. *Nucleic acids research*, *41*(D1), D590-D596. https://doi.org/10.1093/nar/gks1219

Railkin, A. I., Ganf, T. A., & Manylov, O. G. (2004). Marine biofouling: colonization processes and defenses CRC press. *ISBN: 0–8493–1419–4*. https://doi.org/10.1201/9780203503232

Rajala, P., Bomberg, M., Huttunen-Saarivirta, E., Priha, O., Tausa, M., & Carpén, L. (2016). Influence of chlorination and choice of materials on fouling in cooling water system under brackish seawater conditions. *Materials*, *9*(6), 475. https://doi.org/10.3390/ma9060475

Rappé, M. S., Vergin, K., & Giovannoni, S. J. (2000). Phylogenetic comparisons of a coastal bacterioplankton community with its counterparts in open ocean and freshwater systems. *FEMS Microbiology Ecology*, *33*(3), 219-232. https://doi.org/10.1111/j.1574-6941.2000.tb00744.x

Rastelli, E., Dell'Anno, A., Corinaldesi, C., Middelboe, M., Noble, R. T., and Danovaro, R. (2016). Quantification of viral and prokaryotic production rates in benthic ecosystems: a methods comparison. *Front. Microbiol.* 7:1501. https://doi.org/10.3389/fmicb.2016.01501

Rivers, A. R., Weber, K. C., Gardner, T. G., Liu, S., & Armstrong, S. D. (2018). ITSxpress: Software to rapidly trim internally transcribed spacer sequences with quality scores for marker gene analysis. *F1000Research*, *7*. https://doi.org/10.12688/f1000research.15704.1

Rognes, T., Flouri, T., Nichols, B., Quince, C., & Mahé, F. (2016). VSEARCH: a versatile open source tool for metagenomics. *PeerJ*, *4*, e2584. https://doi.org/10.7717/peerj.2584

Russel, J. (2020). MicEco: Various functions for microbial community data. *R package version 0.9*, *9*. https://zenodo.org/badge/latestdoi/83547545

Russell, D. W., & Sambrook, J. (2001). *Molecular cloning: a laboratory manual* (Vol. 1, p. 112). Cold Spring Harbor, NY: Cold Spring Harbor Laboratory.

Sachan, R., & Singh, A. K. (2020). Comparison of microbial influenced corrosion in presence of iron oxidizing bacteria (strains DASEWM1 and DASEWM2). *Construction and Building Materials*, *256*, 119438. https://doi.org/10.1016/J.CONBUILDMAT.2020.119438

Salamone, A. L., Robicheau, B. M., & Walker, A. K. (2016). Fungal diversity of marine biofilms on artificial reefs in the north-central Gulf of Mexico. *Botanica Marina*, *59*(5), 291-305. https://doi.org/10.1515/bot-2016-0032

Salta, M., Wharton, J. A., Blache, Y., Stokes, K. R., & Briand, J. F. (2013). Marine biofilms on artificial surfaces: structure and dynamics. *Environmental microbiology*, *15*(11), 2879-2893. https://doi.org/10.1111/1462-2920.12186

Schroeder, D. M., & Love, M. S. (2004). Ecological and political issues surrounding decommissioning of offshore oil facilities in the Southern California Bight. *Ocean and Coastal Management*, *47*(1–2), 21–48. https://doi.org/10.1016/j.ocecoaman.2004.03.002

Senthilmurugan, B., Radhakrishnan, J. S., Poulsen, M., Tang, L., & AlSaber, S. (2021). Assessment of microbiologically influenced corrosion in oilfield water handling systems using molecular microbiology methods. *Upstream Oil and Gas Technology*, *7*, 100041. https://doi.org/10.1016/J.UPSTRE.2021.100041

Siboni, N., Martinez, S., Abelson, A., Sivan, A., & Kushmaro, A. (2009). Conditioning film and initial biofilm formation on electrochemical CaCO3 deposition on a metallic net in the marine environment. *Biofouling*, *25*(7), 675–683. https://doi.org/10.1080/08927010903097204

Skovhus, T. L., Eckert, R. B., & Rodrigues, E. (2017). Management and control of microbiologically influenced corrosion (MIC) in the oil and gas industry—Overview and a North Sea case study. *Journal of Biotechnology*, *256*, 31–45. https://doi.org/10.1016/J.JBIOTEC.2017.07.003

Skovhus, T. L., Enning, D., & Lee, J. S. (Eds.). (2017). *Microbiologically influenced corrosion in the upstream oil and gas industry*. CRC press.

Stott, J. F. D., & Abdullahi, A. A. (2018). Corrosion in Microbial Environments. *Reference Module in Materials Science and Materials Engineering*. https://doi.org/10.1016/B978-0-12-803581-8.10519-3

Strömberg, S. M., Lundälv, T., & Goreau, T. J. (2010). Suitability of mineral accretion as a rehabilitation method for cold-water coral reefs. Journal of Experimental Marine Biology and Ecology, 395(1–2), 153–161. https://doi.org/10.1016/j.jembe.2010.08.028

Sultana, S. T., Babauta, J. T., & Beyenal, H. (2015). Electrochemical biofilm control: A review. *Biofouling*, *31*(9), 745–758. https://doi.org/10.1080/08927014.2015.1105222

Tang, Y., & Lian, B. (2012). Diversity of endolithic fungal communities in dolomite and limestone rocks from Nanjiang Canyon in Guizhou karst area, China. *Canadian journal of microbiology*, *58*(6), 685-693. https://doi.org/10.1139/w2012-042

Techera, E. J., & Chandler, J. (2015). Offshore installations, decommissioning and artificial reefs: Do current legal frameworks best serve the marine environment? *Marine Policy*, *59*, 53–60. https://doi.org/10.1016/J.MARPOL.2015.04.021

Tornero, V., & Hanke, G. (2016). Chemical contaminants entering the marine environment from sea-based sources: A review with a focus on European seas. *Marine Pollution Bulletin*, *112*(1-2), 17-38. https://doi.org/10.1016/j.marpolbul.2016.06.091

Torsvik, V., Øvreås, L., & Thingstad, T. F. (2002). Prokaryotic Diversity-Magnitude, Dynamics, and Controlling Factors. https://doi.org/10.1126/science.1071698

Trench, R. K. (2012). Electrical Current Stimulates Coral Branching and Growth in Jakarta Bay. In *Innovative Methods of Marine Ecosystem Restoration* (pp. 97-106).

Ulanovskii, I. B., & Ledenev, A. V. (1981). Influence of sulfate-reducing bacteria on cathodic protection of stainless steels. *Prot. Metals*, *17*(2), 169-171.

Un.org. (2021). Retrieved 29 November 2021, from https://www.un.org/depts/los/convention_agreements/texts/unclos/unclos_e.pdf.

Uysal, Z., & Köksalan, İ. (2006). The annual cycle of Synechococcus (cyanobacteria) in the northern Levantine Basin shelf waters (Eastern Mediterranean). *Marine Ecology*, *27*(3), 187-197. https://doi.org/10.1111/j.1439-0485.2006.00105.x

van Elden, S., Meeuwig, J. J., Hobbs, R. J., & Hemmi, J. M. (2019). Offshore Oil and Gas Platforms as Novel Ecosystems: A Global Perspective. In *Frontiers in Marine Science* (Vol. 6). Frontiers Media S.A. https://doi.org/10.3389/fmars.2019.00548

Vargas-Gastélum, L., & Riquelme, M. (2020). The Mycobiota of the Deep Sea: What Omics Can Offer. *Life*, *10*(11), 292. https://doi.org/10.3390/life10110292

Varrella, S., Barone, G., Tangherlini, M., Rastelli, E., Dell'Anno, A., & Corinaldesi, C. (2021). Diversity, Ecological Role and Biotechnological Potential of Antarctic Marine Fungi. *Journal of Fungi*, *7*(5), 391. https://doi.org/10.3390/jof7050391

Victoria, S. N., Sharma, A., & Manivannan, R. (2021). Metal corrosion induced by microbial activity – Mechanism and control options. *Journal of the Indian Chemical Society*, *98*(6), 100083. https://doi.org/10.1016/J.JICS.2021.100083

Wang, H., Ju, L. K., Castaneda, H., Cheng, G., & Newby, B. M. Z. (2014). Corrosion of carbon steel C1010 in the presence of iron oxidizing bacteria Acidithiobacillus ferrooxidans. *Corrosion science*, *89*, 250-257. https://doi.org/10.1016/j.corsci.2014.09.005

White, T. J., Bruns, T., Lee, S. J. W. T., & Taylor, J. (1990). Amplification and direct sequencing of fungal ribosomal RNA genes for phylogenetics. *PCR protocols: a guide to methods and applications*, *18*(1), 315-322. https://doi.org/10.1016/B978-0-12-372180-8.50042-1

Winter, C., Kerros, M. E., & Weinbauer, M. G. (2009). Seasonal and depth-related dynamics of prokaryotes and viruses in surface and deep waters of the northwestern Mediterranean Sea. *Deep Sea Research Part I: Oceanographic Research Papers*, *56*(11), 1972-1982. https://doi.org/10.1016/j.dsr.2009.07.003

Zaccone, R., Azzaro, M., Caruso, G., Crisafi, E., Decembrini, F., Leonardi, M., ... & La Ferla, R. (2019). Effects of climate changes on the microbial activities and prokaryotic abundances in the euphotic layer of the Central Mediterranean Sea. *Hydrobiologia*, *842*(1), 5-30. https://doi.org/10.1007/s10750-019-04023-0

Zardus, J. D., Nedved, B. T., Huang, Y., Tran, C., Hadfield, M. G., & Hadfieldf, M. G. (2008). Microbial Biofilms Facilitate Adhesion in Biofouling Invertebrates. In *Bulletin* (Vol. 214, Issue 1). https://doi.org/10.2307/25066663

Zhou, Z., Wu, T., Liu, M., Wang, B., Li, C., & Yin, F. (2021). Accelerating role of microbial film on soil corrosion of pipeline steel. International Journal of Pressure Vessels and Piping, 192, 104395. https://doi.org/10.1016/j.ijpvp.2021.104395